NASA TECHNICAL NOTE

NASA TN D-4366

THE APERTURE ADMITTANCE OF A GROUND-PLANE-MOUNTED WAVEGUIDE ILLUMINATING A PERFECTLY CONDUCTING SHEET

by J. Earl Jones and C. T. Swift

Langley Research Center
Langley Station, Hampton, Va.

NATIONAL AERONAUTICS AND SPACE ADMINISTRATION • WASHINGTON, D. C. • MARCH 1968

THE APERTURE ADMITTANCE OF A GROUND-PLANE-MOUNTED WAVEGUIDE ILLUMINATING A PERFECTLY CONDUCTING SHEET

By J. Earl Jones and C. T. Swift

Langley Research Center
Langley Station, Hampton, Va.

NATIONAL AERONAUTICS AND SPACE ADMINISTRATION

For sale by the Clearinghouse for Federal Scientific and Technical Information
Springfield, Virginia 22151 – CFSTI price $3.00

THE APERTURE ADMITTANCE OF A GROUND-PLANE-MOUNTED WAVEGUIDE ILLUMINATING A PERFECTLY CONDUCTING SHEET

By J. Earl Jones and C. T. Swift
Langley Research Center

SUMMARY

The Fourier transform technique is applied to derive an expression for the aperture admittance of a ground-plane-mounted, transverse electric and magnetic (TEM) mode-excited parallel-plate waveguide illuminating a perfectly conducting sheet. Based on the aperture admittance expression, an equivalent circuit is developed. It is shown that there is a 1:1 correspondence between elements of the equivalent circuit and higher order modes which exist in the parallel-plate waveguide formed by the ground plane and the reflecting sheet. For the special case where the configuration is treated as a microwave circuit tee junction, the waveguide widths which give the best impedance match are seen to be 0.04 wavelength for the feed guide and 0.03 wavelength for the second guide.

Numerical computations of the reflection coefficient, derived from the aperture admittance, are compared with both the experimental and theoretical results of a similar problem which is solved by application of the geometrical theory of diffraction. General agreement between the two theories except for distances in the vicinity of integral multiples of one half-wavelength is obtained. It is in these regions that strong interactions between the antenna and the reflecting sheet are exhibited. It is believed that the differences in agreement in these regions are due to computational inaccuracies associated with the diffraction theory approach, since it is possible to ascertain the accuracy of the results based on the Fourier transform technique by means of the integral test.

Finally, for various aperture widths, a Smith chart is employed to show that as the distance between the aperture and the reflecting sheet is increased, the admittance locus tends to coalesce about the admittance value for an infinite half-space.

INTRODUCTION

The admittance of an aperture antenna is usually determined, either theoretically or experimentally, under the condition for which the antenna radiates into free space. However, if the antenna is then required to operate in the vicinity of reflecting obstacles,

deviations in the free-space admittance value occur. These deviations are functions of both the aperture geometry and the distance between the aperture and the obstacle.

Early studies of the effect of reflecting obstacles on antennas were concerned with the interaction between antennas and radomes (ref. 1) and with feed antennas for parabolic reflectors (ref. 2). Recent studies have been motivated by a need to relate the properties of a plasma to the admittance of an aperture antenna which radiates into the plasma (refs. 3 to 8).

The problem considered in this paper is the aperture admittance of a ground-plane-mounted, transverse electric and magnetic mode-excited, parallel-plate waveguide illuminating a perfectly conducting sheet located normal to the guide axis. The guide and ground plane may be visualized as two perfectly conducting 90° wedges, the medium being the same on both sides of the aperture. The geometry of this problem is a special case of that treated by Tsai (ref. 8), who employed the geometrical theory of diffraction (refs. 9 to 12) to study the reflection coefficient of parallel-plate waveguides having arbitrary wedge angles. In fact, the inherent advantage of this theory is that geometries for which the wave equation is not separable are readily handled.

For wedge angles of 90°, it is possible to employ the Fourier transform technique to develop an aperture admittance expression where both dielectric-conductor and dielectric-dielectric boundaries may be treated. However, wedge diffraction theory is limited to dielectric-conductor boundaries, since canonical solutions involving dielectric dielectric boundaries are not presently available. Furthermore the Fourier transform technique not only provides a check case for the diffraction theory approach of Tsai, but also allows one to obtain a physical interpretation of mode propagation in the parallel-plate waveguide formed by the ground plane and the reflecting sheet.

In this paper the Fourier transform technique is applied to derive an expression for the aperture admittance, and an equivalent circuit for the aperture is developed. The geometrical configuration is then treated as a parallel-plate waveguide microwave circuit tee junction. Numerical computations of the conductance and the susceptance for this junction are given.

More extensive numerical computations of results are presented next. First, the magnitude and the phase of the reflection coefficient for the 0.278 wavelength aperture are computed and compared with both the experimental and the theoretical results of Tsai. Then, computations of the expression derived by Compton (ref. 5) for the aperture admittance of an infinite medium (that is, the admittance in the absence of the reflecting sheet) are presented. For each of several aperture widths, admittance computations as a function of the reflecting sheet distance are given. The admittance of the same aperture for an infinite medium is also shown for comparison. A particular Fourier transform of importance in this study is evaluated in appendix A. Finally, the problem is reformulated

when the parallel-plate waveguide aperture is replaced by a TE_{10} mode-excited rectangular waveguide. This formulation is presented in appendix B.

SYMBOLS

A	magnetic potential function
$\overline{A}$	Fourier transform of magnetic potential function
a	aperture width
a_n	pole locations of contour integral
B	aperture susceptance
b	normalized aperture susceptance
C_1,C_2,C_3,C_4	arbitrary spectral constants
D_1,D_2,D_3,D_4	particular constants, defined in appendix B
d	distance between aperture plane and reflecting sheet
E	electric field intensity
$\overline{E}$	Fourier transform of electric field intensity
F	electric potential function
$\overline{F}$	Fourier transform of electric potential function
G	aperture conductance
$G(x),G(x,y)$	arbitrary functions
$\overline{G}(k_x),\overline{G}(k_x,k_y)$	Fourier transforms of arbitrary functions
g	normalized aperture conductance
$g(x),g(x_\lambda)$	particular functions, defined in appendix B

H magnetic field intensity

$\overline{H}$ Fourier tranform of magnetic field intensity

$H_0^{(2)}$ Hankel function of second kind and zero order

$h(y), h(y_\lambda)$ particular functions, defined in appendix B

$Im(\ )$ imaginary part of a complex variable

$j = \sqrt{-1}$

$J_0(\ ), K_0(\ ), Y_0(\ )$ Bessel functions

k propagation constant

k' phase shift constant

k'' attenuation constant

M upper summation index

N largest integer satisfying inequality, $N < \frac{2d}{\lambda}$

n mode number; variable of summation

P complex power per unit length (per unit area in appendix B)

p normalized phase-shift constant

q normalized attenuation constant

$Re(\ )$ real part of a complex variable

R_o reflection coefficient (current)

V_o aperture voltage

w complex variable

x,y,z distance along X-, Y- and Z-axes

Y aperture admittance

Y_o characteristic admittance

y normalized aperture admittance

α attenuation constant

β phase-shift constant

γ propagation constant

$\delta_o{}^n = \begin{cases} 0, n \neq 0 \\ 1, n = 0 \end{cases}$ Kronecker delta

ϵ permittivity

θ x-directed propagation constant in absence of reflecting sheet

λ wavelength

μ permeability

$\rho = \sqrt{x^2 + y^2}$

σ conductivity

ω frequency in radians/sec

∇^2 Laplacian operator

Subscripts:

x,y,z measured along respective coordinate axes

λ indicates quantity of length measured in wavelengths

n mode order for parallel-plate waveguide

mn mode order for rectangular waveguide

An asterisk denotes a complex conjugate. An arrow over a symbol denotes a vector quantity and a circumflex denotes a unit vector quantity.

THEORY

Expressions for the aperture admittance and the reflection coefficient of a transverse electric and magnetic (TEM) mode-excited parallel-plate wave-guide opening on to a perfectly conducting ground plane and illuminating a perfectly conducting sheet are derived in this section. The geometry of the problem is shown in figure 1. A parallel-plate waveguide, of width a and infinite in extent in the y-direction, opens on to a perfectly conducting ground plane, infinite in extent in both the x- and y-directions. The coordinate origin lies at the center of the aperture. Located parallel to and spaced a distance d from the aperture plane is a perfectly conducting sheet, infinite in extent in both the x- and y-directions. The medium in both the parallel-plate waveguide and the region between the aperture and the reflecting planes is assumed to be lossless and homogeneous, with permittivity ϵ and permeability μ. One may think of the configuration as being a parallel-plate waveguide of width a feeding a second parallel-plate waveguide of width d.

For the two-dimensional problem under consideration, the fields are assumed to be independent of y. Under this condition, it is readily deduced from Maxwell's two curl equations that the electric and magnetic field components may be decoupled into two independent sets, one transverse electric (TE) and one transverse magnetic (TM) to the Y-axis. A transverse electric and magnetic mode field, the magnetic field being oriented in the y-direction, is assumed to be incident on the aperture from the negative z-direction. Therefore, only the set of components transverse electric to the Y-axis need to be considered in the formulation of the aperture admittance. The time convention $e^{j\omega t}$ is incorporated throughout this paper.

Because of the discontinuity at the aperture, higher order transverse magnetic (TM to the Z-axis) modes, some or all of which may be evanescent, will be induced in the aperture and will tend to propagate back into the waveguide along with the reflected transverse electric and magnetic (TEM) mode. If it is assumed that the aperture width is sufficiently below the cutoff wavelength of the first propagating higher order mode (that is, the TM_2 mode, which propagates for an aperture width of one wavelength), one may then assume that the total aperture electric field consists of only the dominant mode field, that is, the TEM field. The aperture electric field $E_x(x,0)$ is then given by

$$E_x(x,0) = \frac{1}{\sqrt{a}} V_o \tag{1}$$

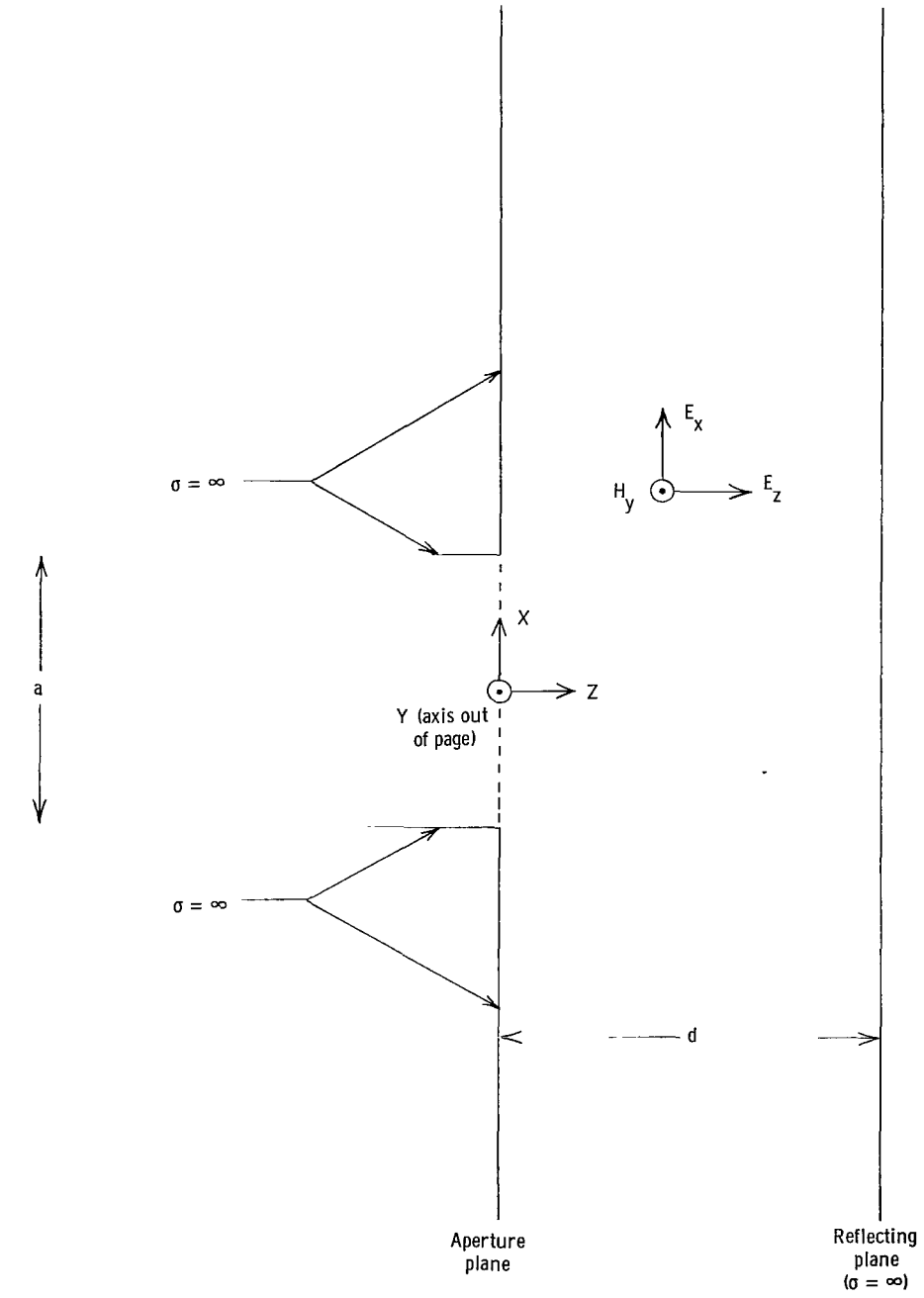

Figure 1.- The ground-plane-mounted parallel-plate waveguide illuminating a reflecting sheet.

where V_o is the root-mean-square aperture voltage. The normalizing factor $\frac{1}{\sqrt{a}}$ is the TEM mode function (see, for example, ref. 13) for the particular waveguide cross section under consideration.

The aperture admittance Y is then given by

$$Y = \frac{P^*}{|V_o|^2} \tag{2}$$

where P is the complex power flow through the aperture per unit length (per meter) in the y-direction and where the asterisk denotes the complex conjugate. In terms of the aperture fields, the aperture admittance is

$$Y = \frac{1}{|V_o|^2} \int_{-a/2}^{a/2} E_x^*(x,0)\, H_y(x,0)\, dx \tag{3}$$

Since the aperture electric field is known (from eq. (1)) the problem is reduced to determining the aperture magnetic field $H_y(x,0)$ arising as a result of the given aperture electric field, or alternatively, determining a relationship between the aperture electric and magnetic fields. This relationship is obtained by solving the boundary value problem for the fields in the region between the aperture and the reflecting planes, and evaluating the results in the aperture plane.

In the region between the aperture and the reflecting planes, the electric field components $E_x(x,z)$ and $E_z(x,z)$ are obtained readily from a knowledge of the magnetic field $H_y(x,z)$ in this region. In particular,

$$E_x(x,z) = -\frac{1}{j\omega\epsilon} \frac{\partial H_y(x,z)}{\partial z} \tag{4}$$

The magnetic field must satisfy the two-dimensional wave equation

$$\frac{\partial^2 H_y(x,z)}{\partial x^2} + \frac{\partial^2 H_y(x,z)}{\partial z^2} + k^2 H_y(x,z) = 0 \tag{5}$$

where

$$k^2 = \omega^2 \mu\epsilon \tag{6}$$

The boundary conditions are: (1) the tangential electric field must vanish on all conducting surfaces, and (2) the tangential electric field on the aperture must be equal to the TEM field, which acts as an equivalent magnetic surface current source for the fields in the region between the aperture and the reflecting planes. Thus,

$$E_x(x,d) = 0 \tag{7}$$

$$\left.\begin{aligned} E_x(x,0) &= \frac{1}{\sqrt{a}} V_o \qquad \left(|x| \leq \frac{a}{2}\right) \\ E_x(x,0) &= 0 \qquad\qquad \left(|x| > \frac{a}{2}\right) \end{aligned}\right\} \tag{8}$$

For the radiation conditions to be met, it is further required that fields propagating in the $\pm x$-directions be either attenuated or phase retarded as $|x|$ increases.

The wave equation may be converted from a partial differential equation to a total differential equation by assuming a Fourier transform[1] solution for $H_y(x,z)$ of the form

$$H_y(x,z) = \frac{1}{2\pi}\int_{-\infty}^{\infty} \overline{H}_y(k_x,z)e^{-jk_x x}\, dk_x \tag{9}$$

Substitution of equation (9) into equation (5) then gives

$$\frac{d^2\overline{H}_y(k_x,z)}{dz^2} + k_z{}^2\overline{H}_y(k_x,z) = 0 \tag{10}$$

where

$$k_z{}^2 = k^2 - k_x{}^2 \tag{11}$$

The general solution of equation (10) is simply

$$\overline{H}_y(k_x,z) = C_1(k_x)e^{jk_z z} + C_2(k_x)e^{-jk_z z} \tag{12}$$

where $C_1(k_x)$ and $C_2(k_x)$ are two arbitrary "spectral constants" to be determined from the boundary conditions (eqs. (7) and (8)). Substituting equation (12) into equation (9) and the result into equation (4) and making use of the Fourier transform definition then establishes

[1] In this paper the one-dimensional Fourier transform pairs $G(x)$ and $\overline{G}(k_x)$ are defined by the relations

$$G(x) = \frac{1}{2\pi}\int_{-\infty}^{\infty} \overline{G}(k_x)e^{-jk_x x}\, dk_x$$

$$\overline{G}(k_x) = \int_{-\infty}^{\infty} G(x)e^{jk_x x}\, dx$$

$$\frac{d\bar{H}_y(k_x,z)}{dz} = -j\omega\epsilon\,\bar{E}_x(k_x,z) \tag{13}$$

or

$$\frac{d\bar{H}_y(k_x,z)}{dz} = -j\omega\epsilon\int_{-\infty}^{\infty} E_x(x,z)e^{jk_x x}\,dx \tag{14}$$

Evaluation of equation (14) at $z = d$ and substitution of equation (7) into the result gives

$$\frac{d\bar{H}_y(k_x,d)}{dz} = 0 \tag{15}$$

Application of equation (12) to equation (15) yields

$$C_2(k_x) = C_1(k_x)e^{j2k_z d} \tag{16}$$

Consequently,

$$\bar{H}_y(k_x,z) = 2C_1(k_x)e^{jk_z d}\cos\left[k_z(z - d)\right] \tag{17}$$

The boundary condition (eq. (8)) is used to determine the remaining spectral constant. Substitution of equation (17) into equation (13) and evaluating the result at $z = 0$ gives

$$C_1(k_x) = -\frac{j\omega\epsilon\bar{E}_x(k_x,0)}{2k_z e^{jk_z d}\sin(k_z d)} \tag{18}$$

Hence

$$\bar{H}_y(k_x,z) = -\frac{j\omega\epsilon\bar{E}_x(k_x,0)\cos\left[k_z(z - d)\right]}{k_z\sin(k_z d)} \tag{19}$$

where

$$\bar{E}_x(k_x,0) = \int_{-a/2}^{a/2} E_x(x,0)\,e^{jk_x x}\,dx \tag{20}$$

Substituting equation (8) into equation (20) gives

$$\bar{E}_x(k_x,0) = V_o\sqrt{a}\,\frac{\sin\left(\frac{k_x a}{2}\right)}{\frac{k_x a}{2}} \tag{21}$$

Evaluating equation (19) at $z = 0$ yields the aperture magnetic field transform in terms of the aperture electric field transform, that is,

$$H_y(k_x,0) = - \frac{j\omega\epsilon \overline{E}_x(k_x,0)}{k_z \tan(k_z d)} \tag{22}$$

The aperture admittance as given by equation (3) may be found by substituting equation (21) into equation (22), performing the indicated inverse transform to obtain $H_y(x,0)$, and then substituting the result, along with equation (1), into equation (3) and performing the integration over the aperture. However, it is convenient to use an alternate approach (ref. 5, p. 22) to obtain an expression for the aperture admittance. Since by equation (8) the tangential electric field must vanish on the ground plane, the limits of integration on equation (3) may be extended to infinity without affecting the result. Then by Parseval's theorem[2], equation (3) becomes

$$Y = \frac{1}{2\pi |V_o|^2} \int_{-\infty}^{\infty} \overline{E}_x{}^*(k_x,0)\, \overline{H}_y(k_x,0)\, dk_x \tag{23}$$

Substitution of equation (22) into equation (23) then yields the result

$$Y = - \frac{j\omega\epsilon}{2\pi |V_o|^2} \int_{-\infty}^{\infty} \frac{|\overline{E}_x(k_x,0)|^2}{k_z \tan(k_z d)} dk_x \tag{24}$$

which becomes, upon substitution of equation (21),

$$Y = - \frac{j\omega\epsilon a}{2\pi} \int_{-\infty}^{\infty} \frac{\sin^2\left(\frac{k_x a}{2}\right)}{\left(\frac{k_x a}{2}\right)^2 k_z \tan(k_z d)} dk_x \tag{25}$$

[2]For the Fourier transform pairs

$$G_1(x) = \frac{1}{2\pi} \int_{-\infty}^{\infty} \overline{G}_1(k_x)\, e^{-jk_x x}\, dk_x$$

$$G_2(x) = \frac{1}{2\pi} \int_{-\infty}^{\infty} \overline{G}_2(k_x)\, e^{-jk_x x}\, dk_x$$

Parseval's theorem states

$$\int_{-\infty}^{\infty} G_1(x)\, G_2{}^*(x)\, d_x = \frac{1}{2\pi} \int_{-\infty}^{\infty} \overline{G}_1(k_x)\, \overline{G}_2{}^*(k_x)\, dk_x$$

This integrand may be rearranged and Parseval's theorem may be used again. Let

$$\overline{G}_1(k_x) = \frac{1}{k_z \tan(k_z d)} \tag{26}$$

$$\overline{G}_2{}^*(k_x) = \overline{G}_2(k_x) = \frac{\sin^2\left(\frac{k_x a}{2}\right)}{\left(\frac{k_x a}{2}\right)^2} \tag{27}$$

By definition of the inverse transform

$$G_2{}^*(x) = G_2(x) = \frac{1}{2\pi}\int_{-\infty}^{\infty} \frac{\sin^2\left(\frac{k_x a}{2}\right)}{\left(\frac{k_x a}{2}\right)^2} e^{-jk_x x}\, dk_x \tag{28}$$

This integral is evaluated by residue theory. The result, as given by Compton (ref. 5, p. 24), is

$$\left.\begin{aligned} G_2{}^*(x) = G_2(x) &= \frac{1}{a^2}(a - |x|) \qquad (|x| \leq a) \\ G_2{}^*(x) = G_2(x) &= 0 \qquad\qquad\quad (|x| > a) \end{aligned}\right\} \tag{29}$$

Similarly,

$$G_1(x) = \frac{1}{2\pi}\int_{-\infty}^{\infty} \frac{e^{-jk_x x}}{k_z \tan(k_z d)}\, dk_x \tag{30}$$

The integral in equation (30) is also evaluated by residue theory. Because this integral admits to physical interpretation, details of the evaluation of this integral are given and are discussed in appendix A. The requirements for the behavior of the fields for large $|x|$ are taken into account in appendix A. It is found that the poles of the integrand, namely,

$$k_z = \pm\left(\frac{n\pi}{d}\right) \qquad (n = 0, 1, 2, \ldots) \tag{31}$$

give rise to discrete waveguide modes (transverse magnetic to the x-direction) which propagate in the $\pm x$-directions. From appendix A, the inverse transform in equation (30) is

$$G_1(x) = \frac{j}{d} \sum_{n=0}^{\infty} \frac{e^{-jk_x|x|}}{\left(1 + \delta_o{}^n\right)k_x} \tag{32}$$

where $\delta_o{}^n$ is the Kronecker delta; that is,

$$\left.\begin{aligned} \delta_o{}^n &= 1 \qquad (n = 0) \\ \delta_o{}^n &= 0 \qquad (n \neq 0) \end{aligned}\right\} \tag{33}$$

and where the waveguide modes k_x are now dependent on n and are given by

$$\left.\begin{aligned} k_x &= +\sqrt{k^2 - \left(\frac{n\pi}{d}\right)^2} \qquad \left(k^2 > \left(\frac{n\pi}{d}\right)^2\right) \\ k_x &= -j\sqrt{\left(\frac{n\pi}{d}\right)^2 - k^2} \qquad \left(k^2 < \left(\frac{n\pi}{d}\right)^2\right) \end{aligned}\right\} \tag{34}$$

that is, the correct branch of k_x, as defined implicitly by equation (11), is chosen to insure proper behavior of the fields for large $|x|$.

Then by use of Parseval's theorem, equation (25) becomes

$$\left.\begin{aligned} Y &= -j\omega\epsilon a \int_{-\infty}^{\infty} G_1(x)G_2{}^*(x)\, dx \\ Y &= -\, j\omega\epsilon a \int_{-a}^{a} \left[\frac{1}{a^2}(a - |x|)\right] \left[\frac{j}{d} \sum_{n=0}^{\infty} \frac{e^{-jk_x|x|}}{\left(1 + \delta_o{}^n\right)k_x}\right] dx \end{aligned}\right\} \tag{35}$$

which upon rearranging and taking advantage of the evenness of the integrand integrated over a symmetric interval, becomes

$$Y = \frac{2\omega\epsilon}{ad} \sum_{n=0}^{\infty} \left[\frac{1}{\left(1 + \delta_o{}^n\right)} \int_0^a \frac{(a - x)e^{-jk_x x}}{k_x}\, dx\right] \tag{36}$$

The integral in equation (36) is easily evaluated and the result is

$$\int_0^a \frac{(a - x)e^{-jk_x x}}{k_x}\, dx = \frac{1}{k_x{}^3}\left\{\left[1 - \cos(k_x a)\right] - j\left[(k_x a) - \sin(k_x a)\right]\right\} \tag{37}$$

Using equation (37) in equation (36) yields

$$Y = \frac{2\omega\epsilon}{ad} \sum_{n=0}^{\infty} \left(\frac{1}{\left(1 + \delta_o{}^n\right) k_x{}^3} \left\{ \left[1 - \cos(k_x a) \right] - j \left[(k_x a) - \sin(k_x a) \right] \right\} \right) \tag{38}$$

where the values of k_x are as given by equation (34).

The expression in equation (38) may be manipulated into the form

$$Y = G + jB \tag{39}$$

where G is the conductance and B is the susceptance by letting

$$\beta_n = \sqrt{k^2 - \left(\frac{n\pi}{d}\right)^2} \qquad \left(k^2 > \left(\frac{n\pi}{d}\right)^2\right) \tag{40}$$

$$\alpha_n = \sqrt{\left(\frac{n\pi}{d}\right)^2 - k^2} \qquad \left(k^2 < \left(\frac{n\pi}{d}\right)^2\right) \tag{41}$$

and N be the largest integer such that the following inequality holds:

$$N < \frac{2d}{\lambda} \tag{42}$$

where

$$\lambda = \frac{2\pi}{k} \tag{43}$$

Then for k_x real, $k_x = \beta_n$; whereas for k_x imaginary, $k_x = -j\alpha_n$. By using these substitutions in equation (38) and rearranging, one finally obtains

$$Y = \frac{2\omega\epsilon}{ad} \left(\sum_{n=0}^{N} \left[\frac{1 - \cos(\beta_n a)}{\left(1 + \delta_o{}^n\right) \beta_n{}^3} \right] - j \left\{ \sum_{n=0}^{N} \left[\frac{(\beta_n a) - \sin(\beta_n a)}{\left(1 + \delta_o{}^n\right) \beta_n{}^3} \right] + \sum_{n=N+1}^{\infty} \left[\frac{1 - (\alpha_n a) - e^{-\alpha_n a}}{\left(1 + \delta_o{}^n\right) \alpha_n{}^3} \right] \right\} \right) \tag{44}$$

Hence

$$G = \frac{2\omega\epsilon}{ad} \sum_{n=0}^{N} \left[\frac{1 - \cos(\beta_n a)}{\left(1 + \delta_o{}^n\right) \beta_n{}^3} \right] \tag{45}$$

$$B = -\frac{2\omega\epsilon}{ad} \left(\sum_{n=0}^{N} \left[\frac{(\beta_n a) - \sin(\beta_n a)}{\left(1 + \delta_o{}^n\right) \beta_n{}^3} \right] + \sum_{n=N+1}^{\infty} \left[\frac{1 - (\alpha_n a) - e^{-\alpha_n a}}{\left(1 + \delta_o{}^n\right) \alpha_n{}^3} \right] \right) \tag{46}$$

For purposes of numerical computations, it is convenient to normalize equation (44). Let

$$a_\lambda = \frac{a}{\lambda} \tag{47}$$

$$d_\lambda = \frac{d}{\lambda} \tag{48}$$

$$p_n = \frac{\beta_n}{k} = \sqrt{1 - \left(\frac{n}{2d_\lambda}\right)^2} \qquad \left(n < 2d_\lambda\right) \tag{49}$$

$$q_n = \frac{\alpha_n}{k} = \sqrt{\left(\frac{n}{2d_\lambda}\right)^2 - 1} \qquad \left(n > 2d_\lambda\right) \tag{50}$$

and let

$$y = \frac{Y}{Y_o} = \frac{G + jB}{Y_o} = g + jb \tag{51}$$

where Y_o is the characteristic admittance of the medium, that is,

$$Y_o = \frac{\omega\epsilon}{k} \tag{52}$$

and where y, g, and b are the normalized aperture admittance, conductance, and susceptance, respectively. Then one obtains

$$g = \frac{1}{(2\pi^2)a_\lambda d_\lambda} \sum_{n=0}^{N} \left[\frac{1 - \cos(2\pi p_n a_\lambda)}{\left(1 + \delta_o{}^n\right)p_n{}^3}\right] \tag{53}$$

$$b = -\frac{1}{(2\pi^2)a_\lambda d_\lambda}\left\{\sum_{n=0}^{N}\left[\frac{\left(2\pi p_n a_\lambda\right) - \sin\left(2\pi p_n a_\lambda\right)}{\left(1 + \delta_o{}^n\right)p_n{}^3}\right] + \sum_{n=N+1}^{\infty}\left[\frac{1 - \left(2\pi q_n a_\lambda\right) - e^{-2\pi q_n a_\lambda}}{\left(1 + \delta_o{}^n\right)q_n{}^3}\right]\right\} \tag{54}$$

The reflection coefficient R_o (current) may then be found from the expression

$$R_o = \frac{y - 1}{y + 1} \tag{55}$$

Convergence of the infinite series in equation (54) is readily established by means of the integral test, which may also be used to compute the susceptance to any desired

accuracy. The rapidity of convergence is dictated by the second term in the infinite series.

Based on the normalized equations (47) to (55), a digital computer program was written to perform computations of reflection coefficient and aperture admittance for selected values of a_λ and d_λ. In the computer program the infinite summation index in equation (54) was replaced by a finite summation index M which was chosen to be $200d_\lambda$. The accuracy of the resulting computations was determined to be approximately 1 percent, which is at least as accurate as one might hope to achieve experimentally.

RESULTS AND DISCUSSION

An Equivalent Circuit

A useful equivalent circuit, readily amenable to physical interpretation, may be derived from equations (53) and (54). From these equations, it is revealed that the conductance consists of the sum of a finite number of terms; whereas, the susceptance consists of the sum of an infinite number of terms. Thus, one equivalent circuit for the aperture is a one terminal-pair network consisting of a finite number of conductance elements and an infinite number of susceptance elements, all elements being in parallel.

An interesting relationship exists between the circuit elements and the higher order modes present in the parallel-plate waveguide formed by the ground plane and the reflecting sheet. These modes, transverse magnetic to the x-direction, were mentioned earlier in connection with the evaluation of the integral in equation (30). For reflecting sheet distances less than one half-wavelength, there is only one term in the expression for the conductance; that is, there is only one conductance element. Likewise, only one mode (the mode transverse electric and magnetic to the x-direction) propagates in this guide, whereas the higher order TM modes are all evanescent. However, as the reflecting sheet distance is increased, a new term is added to the conductance expression (and a new conductance element to the circuit) each time the reflecting distance passes through an integral multiple of a half-wavelength, that is, whenever a new mode begins to propagate. (For brevity, the half-wavelength distances will be hereafter denoted as "the critical distances.") Moreover, each of the propagating modes contributes one susceptance element. However, the evanescent modes contribute only a susceptance element, as might be anticipated on physical grounds since these modes represent reactive energy storage. The equivalent circuit is shown in figure 2.

As seen from equations (53) and (54), both the conductance and the susceptance become infinite at the critical distances, because of the infinite value of the particular conductance and susceptance elements representing the mode which begins to propagate at the corresponding critical distance. Physically, this condition implies that the

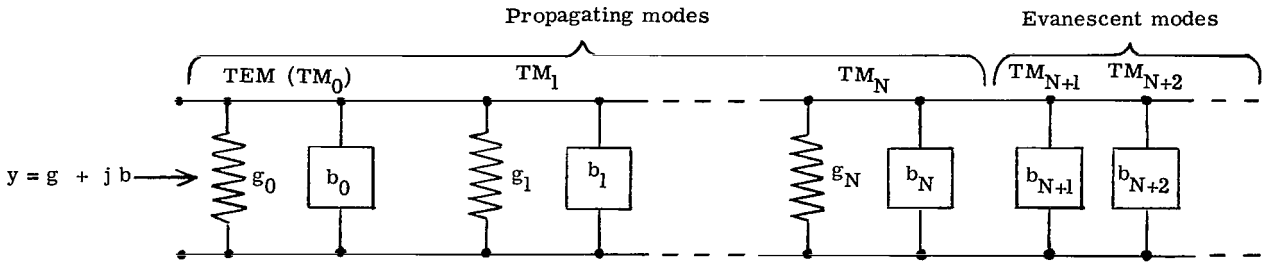

Figure 2.- Equivalent circuit of the aperture.

reflecting sheet behaves like a short circuit (infinite conductance), and the walls of the parallel-plate waveguide of width a may as well be transferred in the positive z-direction a distance d (infinite susceptance) to again come in contact with the reflecting sheet. Phenomena occurring at the critical distances are discussed later in more detail.

The Tee Junction

If the reflecting sheet distance is restricted to values less than one half-wavelength and the aperture width to values less than one wavelength, then only the dominant mode propagates. From the microwave circuit viewpoint, the configuration is a parallel-plate waveguide tee junction.

Numerical computations of the normalized aperture conductance and susceptance as functions of the aperture width and for fixed values of the reflecting sheet distance were performed and are presented in figure 3. It is seen from this figure that the normalized conductance is a maximum for an aperture width of 0.37 wavelength. This result may be deduced analytically by differentiating the conductance expression obtained from equation (53), namely,

$$g = \frac{1}{2\pi d_\lambda}\left[\frac{\sin^2(\pi a_\lambda)}{\pi a_\lambda}\right] \qquad \left(0 \leqq d_\lambda < 0.5\right) \qquad (56)$$

and setting the result equal to zero. The results in figure 3 may also be used to obtain waveguide dimensions for the best impedance match, which occurs for a normalized conductance of 1 and a normalized susceptance of zero. This condition is fulfilled for a feed guide width a_λ of 0.04 wavelength and for the width d_λ of the second guide of 0.03 wavelength.

It is also noted that the conductance is zero for aperture widths of one wavelength and for reflecting sheet distances between 0 and 0.5 wavelength. This result may be deduced from the following physical observation. If one may think of the two corners of the two wedges as line currents fed out of phase, there will be a net cancellation of the

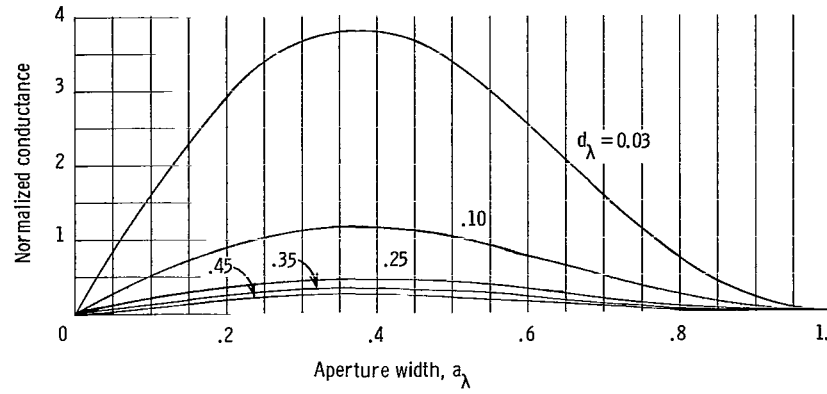

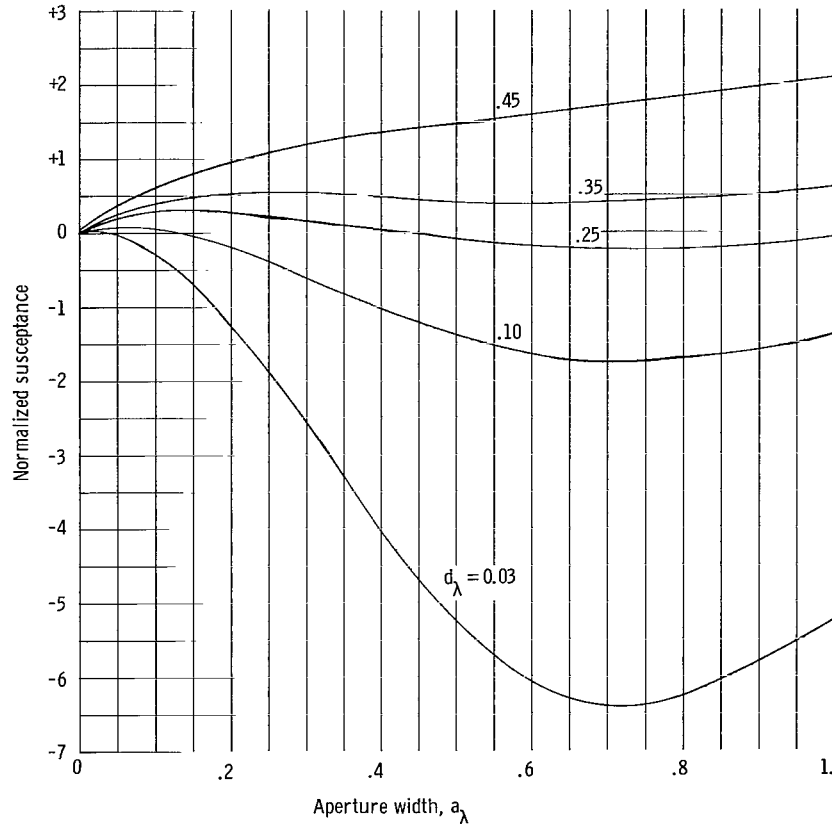

Figure 3.- The normalized conductance and the normalized susceptance as a function of the aperture width for the ground-plane-mounted parallel-plate waveguide illuminating a reflecting sheet.

radiation field in the $\pm x$-directions in the region between the ground plane and the reflecting sheet. However, it is believed that results for this aperture width would be modified if the influence of the TM_2 mode, which begins propagating back into the guide for this aperture width, is included in the formulation.

Comparison of Fourier Transform Solution With Diffraction Theory Solution

Computations of the magnitude and the phase of the reflection coefficient as a function of the reflecting sheet distance for a 0.278-wavelength aperture were performed in order to check the Fourier transform solution with the diffraction theory approach of Tsai. These results are presented in figures 4 and 5.

General agreement among the Fourier transform technique, the diffraction theory approach, and the experimental measurements is obtained, except for reflecting sheet distances in the vicinity of the critical distances. In figure 4, computations based on the Fourier transform technique indicate that the reflection coefficient magnitude is very sensitive with respect to the reflecting sheet distance for values in the vicinity of the critical distances. It is also evident that as the reflecting sheet distance is increased, the sensitivity becomes much more enhanced. In any event, the reflecting sheet will always have an effect on the reflection coefficient, no matter how large the spacing. The parallel-plate waveguide formed by the ground plane and the reflecting sheet is essentially a one-dimensional cavity resonator. The configuration may also be thought of as a simplified version of a Fabry-Perot resonator with a single aperture feed. Both theoretical and experimental studies of microwave Fabry-Perot interferometers have been reported in references 14 to 18.

Although both the experimental and the theoretical data of Tsai are in agreement for any reflecting sheet distance, both are believed to be in error in the vicinity of the critical distances. The theoretical data are believed to be in error because of an insufficient number of bounce waves included in the formulation; whereas, the experimental data are believed to be limited by diffraction losses.

In both figures 4 and 5, the number of maxima and minima per half-wavelength for the diffraction theory data corresponds to the number of bounce waves (4) included in the computations. Possibly the diffraction theory curve would become smoother (and the peaks at each half-wavelength much higher) as the number of bounce waves included is increased.

The theoretical model is believed to represent inadequately the experimental model in the vicinity of the critical distances because of diffraction losses, which occur basically for two reasons: (a) approximation of the infinite conducting planes by finite size planes, and (b) misalinement of the conducting planes from parallelism (ref. 18, p. 63). Diffraction losses are increased as the reflecting sheet distance is increased, but for a given distance are reduced as the ground and the reflecting planes are enlarged (ref. 18, pp. 63-64).

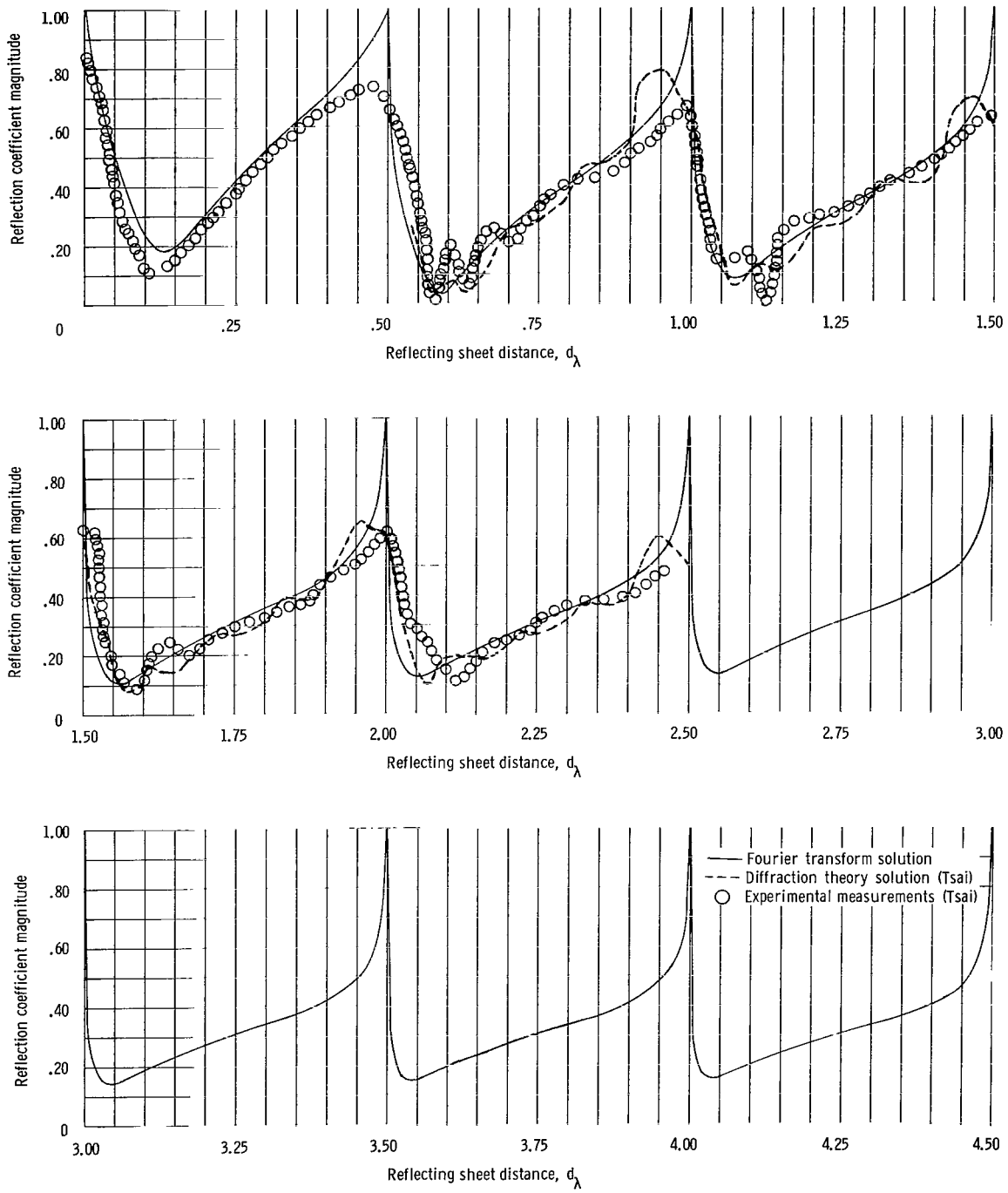

Figure 4.- The variation of reflection coefficient magnitude with the reflecting sheet distance for an aperture width of 0.278 wavelengths.

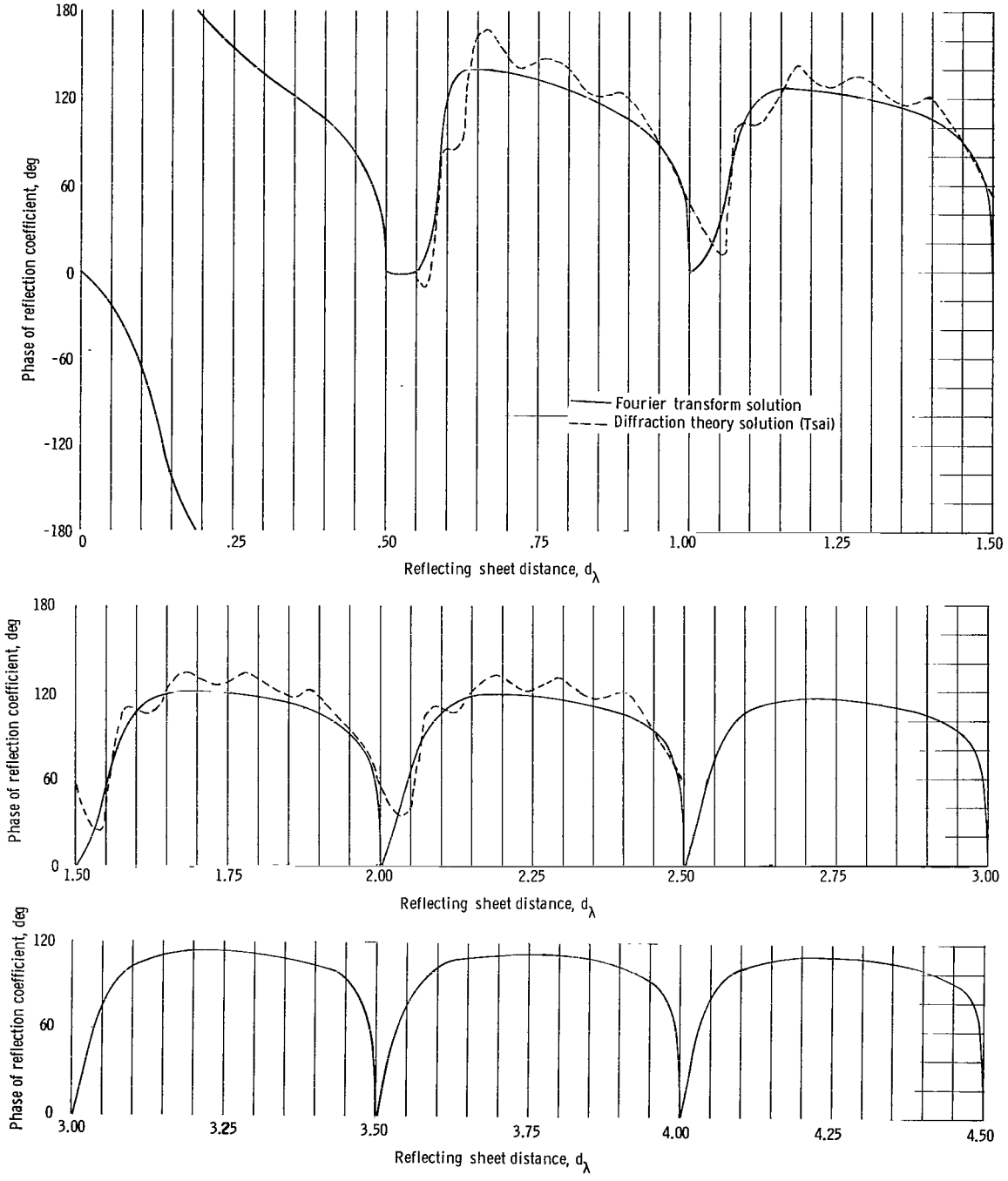

Figure 5.- The variation of reflection coefficient phase with the reflecting sheet distance for an aperture width of 0.278 wavelengths.

In any event, it is believed that conductor and dielectric losses do not markedly contribute to a lowering of the reflection coefficient at the critical distances. However, smooth, highly conducting, low loss surfaces such as silver are certainly desirable (ref. 14, p. 222). Although dielectric losses in the medium between the ground and the reflecting planes would tend to reduce the reflection coefficient at the critical distances[3], it is believed that for a medium such as air, the effect is negligible. For example, for Fabry-Perot interferometers with air as a dielectric, Culshaw (ref. 16, p. 135) has obtained power reflection coefficients of 0.999 at critical distances for reflecting sheet spacings of 25 wavelengths, and Q values on the order of 300 000.

Results of Aperture Admittance Computations

Before considering the aperture admittance computations for the ground-plane-mounted parallel-plate guide illuminating the reflecting sheet other than the computations presented earlier, it is interesting first to consider the aperture admittance of the same guide with the reflecting sheet absent. For this case, the medium is then a lossless half-space. For the same modal voltage $\frac{V_0}{\sqrt{a}}$ and for the case where the medium is the same on both sides of the aperture, the admittance is then a special case of the result derived by Compton (ref. 5, p. 25). In normalized form, this result is

$$y = \frac{2\pi}{a_\lambda} \int_0^{a_\lambda} (a_\lambda - x_\lambda) H_0^{(2)}(2\pi x_\lambda)\, dx_\lambda \tag{57}$$

Equation (57) was programed for numerical computations on a digital computer. The results are presented on a Smith chart for reference purposes in figure 6.

Computations of the normalized aperture admittance with the reflecting sheet present were then performed for four aperture widths (0.100, 0.278, 0.600, and 1.000 wavelengths) over the range of values for which no propagating higher order modes are reflected back into the waveguide (although the TM_2 mode is on the verge of propagating for an aperture width of 1.000 wavelength). These computations are shown on Smith charts in figure 7. The infinite medium point for the particular aperture width was taken from the admittance locus in figure 6.

Several interesting observations may be deduced from figure 7. First, it is seen that as the reflecting sheet spacing is increased, the admittance locus tends to coalesce about the infinite medium point predicted by Compton. Second, the sensitivity of the

[3]In appendix A, it is seen that the assumption of a slight loss causes the poles of the contour integral associated with the aperture admittance to shift off-axis. This condition results in residues that, although large, are nevertheless finite.

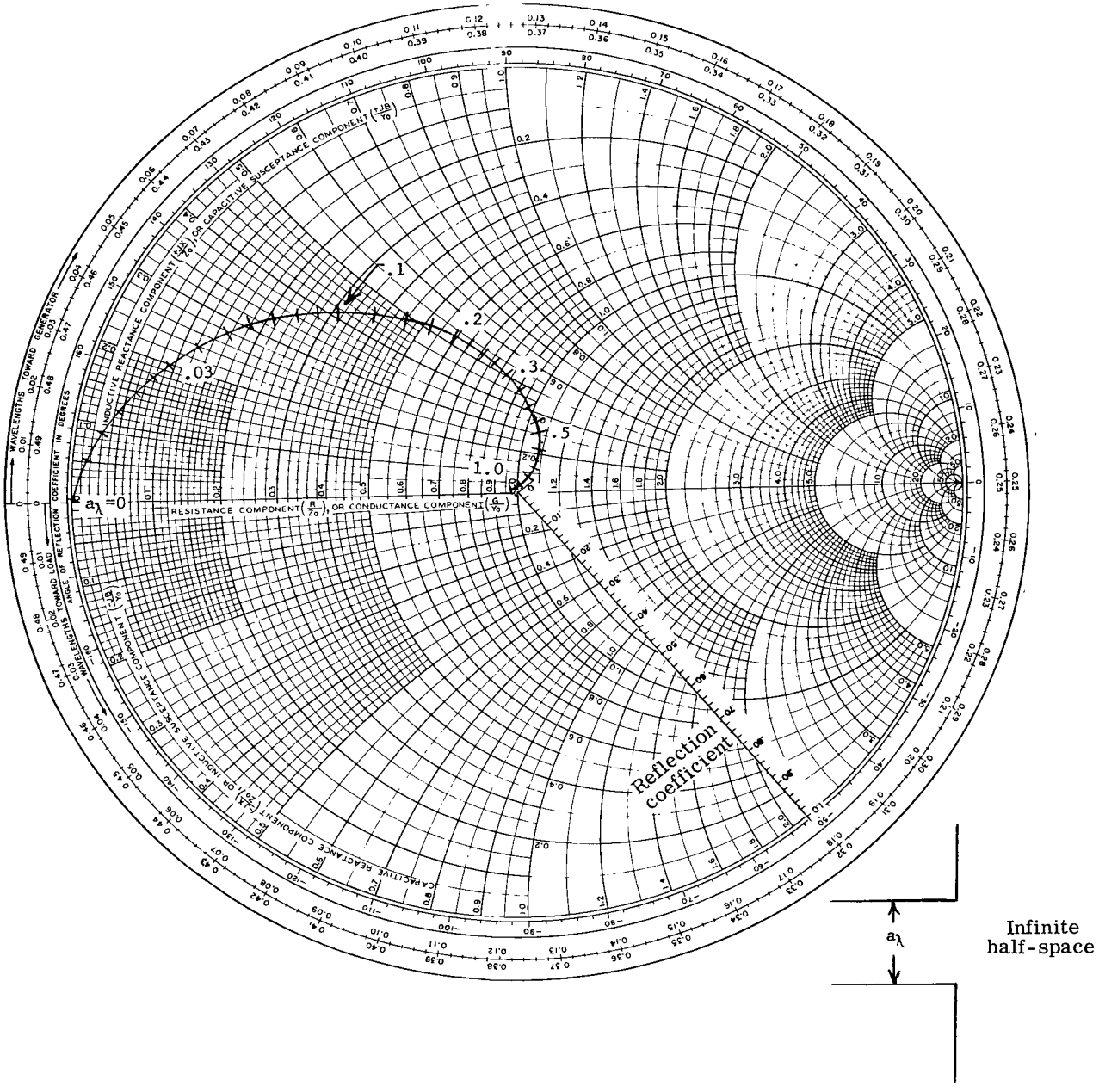

Figure 6.- The normalized aperture admittance of a ground-plane-mounted parallel-plate waveguide radiating into a lossless infinite half-space (after Compton, ref. 5, p. 25).

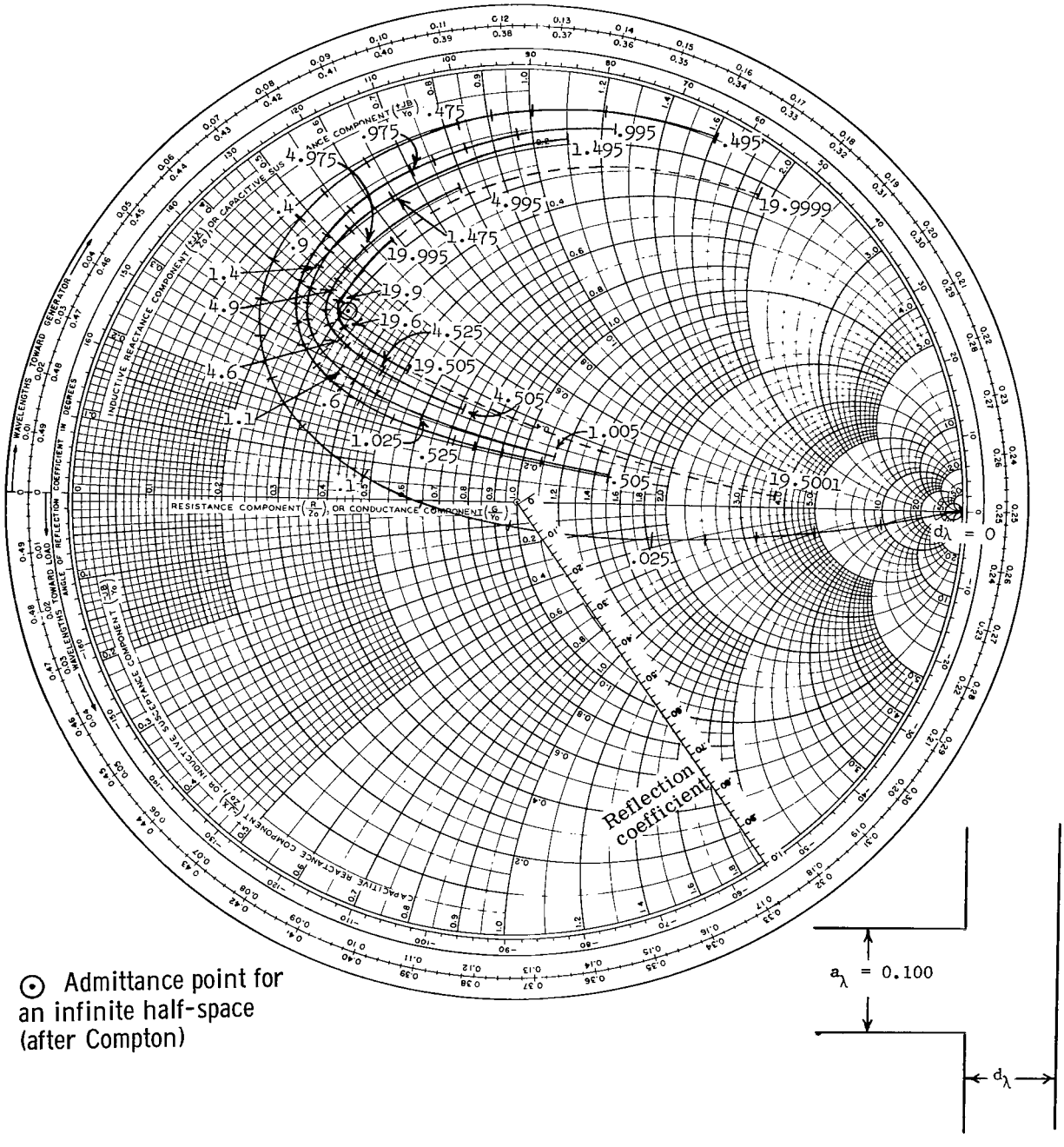

Figure 7.- The normalized aperture admittance of a ground-plane-mounted parallel-plate waveguide illuminating a reflecting sheet, for various aperture widths.

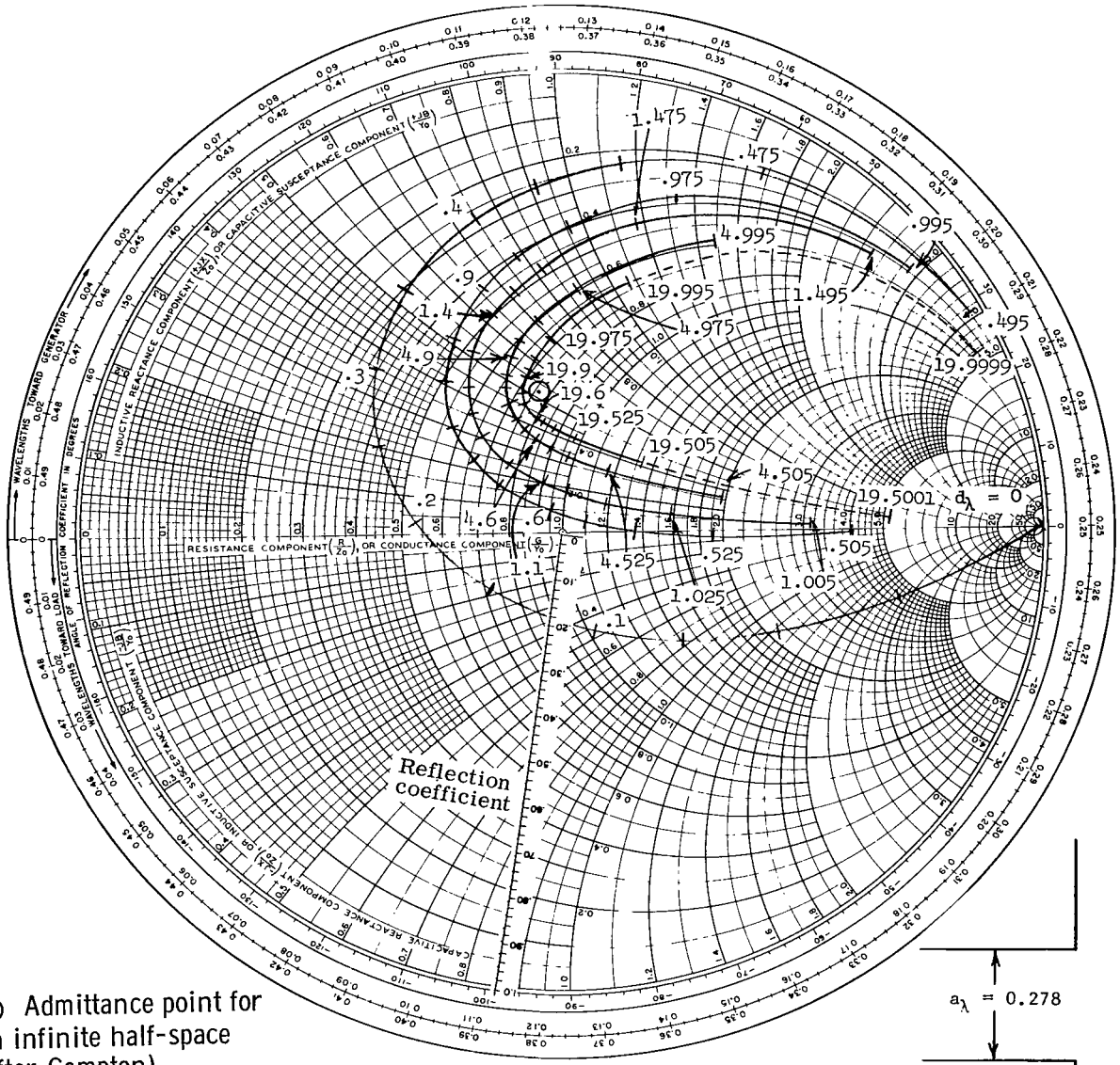

⊙ Admittance point for an infinite half-space (after Compton)

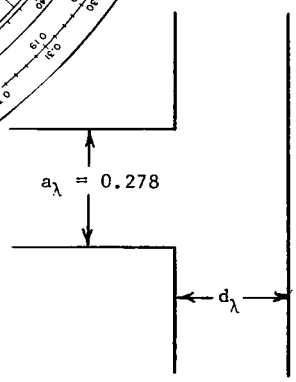

Figure 7.- Continued.

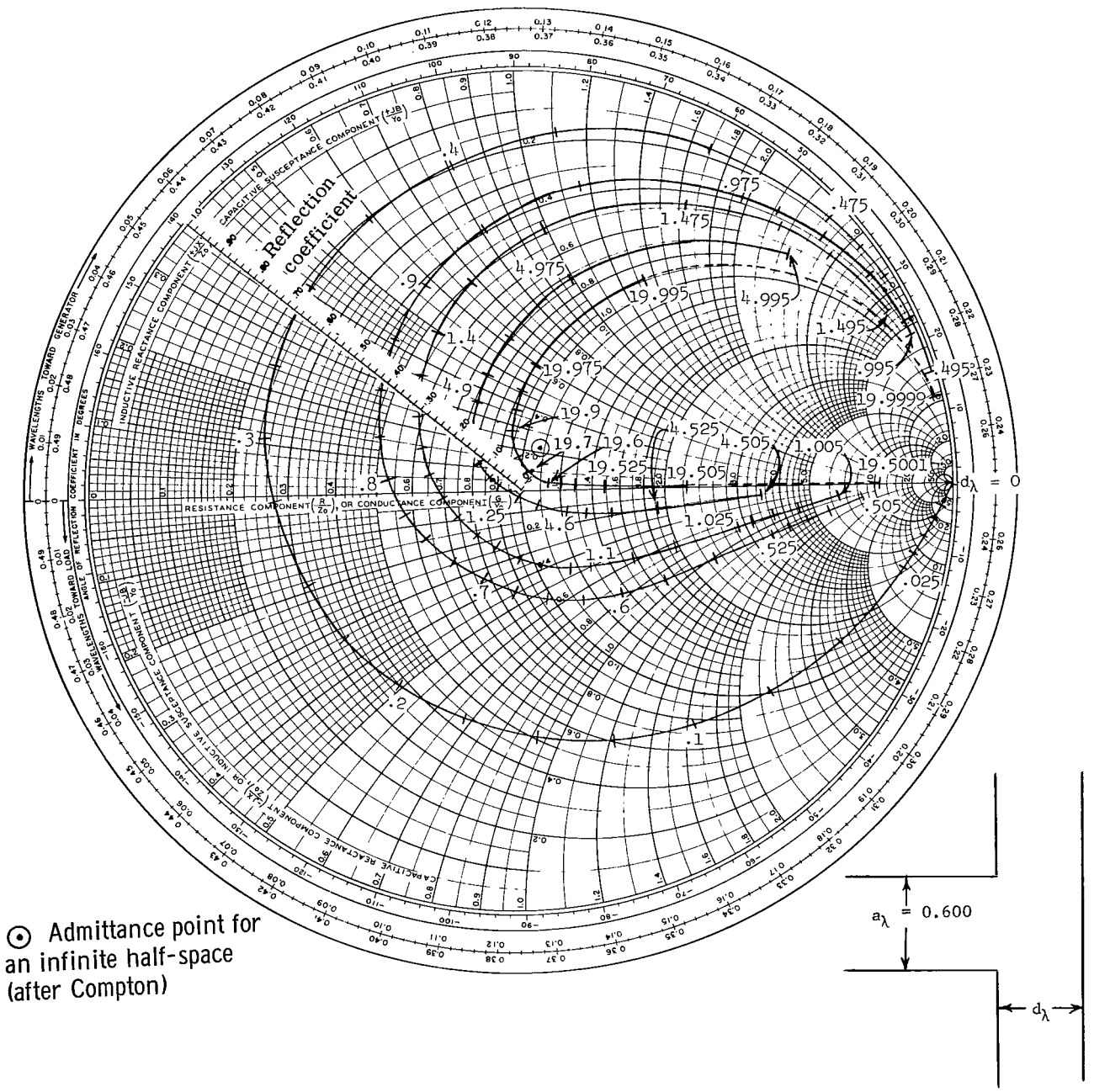

⊙ Admittance point for an infinite half-space (after Compton)

Figure 7.- Continued.

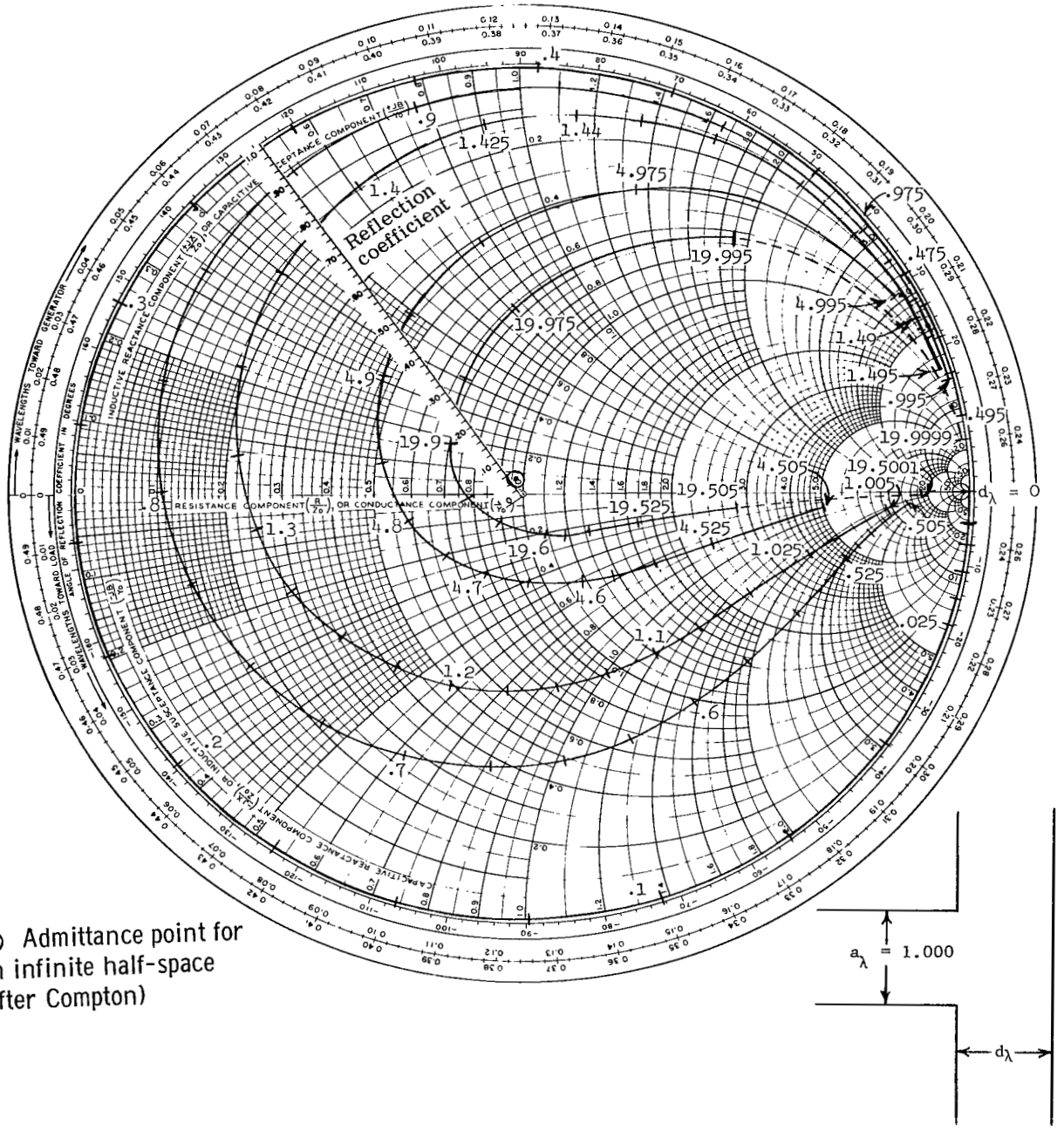

⊙ Admittance point for an infinite half-space (after Compton)

Figure 7.- Concluded.

reflection coefficient with distance in the vicinity of the critical distances is evident on the admittance loci. Finally, it is noted that, for large distances, the susceptance is essentially independent of distances slightly greater than critical; whereas, the conductance is practically independent of distance for distances slightly less than critical. In any event, as already pointed out, the reflecting sheet theoretically will always have an effect on the aperture admittance no matter how large the reflecting sheet spacing, although the tolerances become extremely critical as the spacing is increased.

CONCLUDING REMARKS

The aperture admittance of a ground-plane-mounted, transverse electric and magnetic mode-excited parallel-plate waveguide illuminating a perfectly conducting sheet was derived by a Fourier transform technique. It was shown that a 1:1 correspondence exists between the elements of an equivalent circuit, which was developed from the admittance expression, and higher order modes present in the parallel-plate waveguide formed by the ground plane and the reflecting sheet. For the special case where the configuration was treated as a microwave circuit tee junction, the waveguide widths which give the best impedance match were seen to be 0.04 wavelength for the feed guide and 0.03 wavelength for the second guide.

Numerical computations of the reflection coefficient, derived from the aperture admittance, were compared with both the experimental and theoretical results of a similar problem which is solved by application of the geometrical theory of diffraction. General agreement between the two theories was obtained, except for distances in the vicinity of integral multiples of one half-wavelength. It is in these regions that strong interactions between the antenna and the reflecting sheet were seen to occur. It is believed that the differences in agreement in these regions are due to computational inaccuracies associated with the diffraction theory approach, since it is possible to ascertain the accuracy of the results based on the Fourier transform technique by means of the integral test.

Finally, for various aperture widths, a Smith chart was employed to show that as the distance between the aperture and the reflecting sheet is increased, the admittance locus tends to coalesce about the admittance value for an infinite half-space.

Langley Research Center,
National Aeronautics and Space Administration,
Langley Station, Hampton, Va., June 21, 1967,
125-22-02-02-23.

APPENDIX A

EVALUATION OF AN INVERSE FOURIER TRANSFORM

Because of the physical interpretation associated with the Fourier transform $G_1(x)$ given in equation (30) (and in equation (B53) in an analogous treatment of the rectangular waveguide aperture), it seems desirable to discuss the evaluation of this Fourier transform in more detail. The integral to be evaluated is

$$G(x) = \frac{1}{2\pi} \int_{-\infty}^{\infty} \frac{1}{k_z \tan(k_z d)} e^{-jk_x x} \, dk_x \tag{A1}$$

where k_z is defined implicitly by the relation[4]

$$k_x^2 = k^2 - k_y^2 - k_z^2 \tag{A2}$$

or by

$$k_x^2 = \theta^2 - k_z^2 \tag{A3}$$

where

$$\theta^2 = k^2 - k_y^2 \tag{A4}$$

It is to be noted that θ^2 is real for a lossless medium.

The integral in equation (A1) may be evaluated by means of residue theory. Let a complex variable w be defined such that $\mathrm{Re}[w] = k_x$ and consider, in the complex w-plane, the contour integral

$$G(x) = \int_C \frac{1}{k_{wz} \tan(k_{wz} d)} e^{-jwx} \, dw \tag{A5}$$

where

$$w^2 = \theta^2 - k_{wz}^2 \tag{A6}$$

and where $k_{wz}^2 = k_z^2$ wherever $w^2 = k_x^2$. The path of integration in the w-plane is then along the real axis, from $-\infty$ to ∞.

---

[4]The term k_y^2 is required to evaluate equation (B53) because of the three-dimensional nature of the problem in appendix B. For equation (30), however, $k_y^2 = 0$ throughout appendix A.

APPENDIX A

The integral in equation (A5) is of the form

$$G(x) = \int_C f(w) e^{-jwx}\, dw \tag{A7}$$

where

$$f(w) = \frac{1}{k_{wz} \tan(k_{wz} d)} \tag{A8}$$

Consideration of the expansion

$$\frac{1}{k_{wz} \tan(k_{wz} d)} = -\frac{2}{d} \sum_{n=0}^{\infty} \frac{1}{(1 + \delta_o{}^n)\left\{w^2 - \left[\theta^2 - \left(\frac{n\pi}{d}\right)^2\right]\right\}} \tag{A9}$$

reveals that there are no branch points in the w-plane. Furthermore, the poles of $f(w)$ are simple except as subsequently noted, and occur for values of k_{wz} which satisfy the relation

$$k_{wz} d = n\pi \qquad (n = 0, 1, 2, \ldots) \tag{A10}$$

from which

$$w^2 = \theta^2 - \left(\frac{n\pi}{d}\right)^2 \tag{A11}$$

There are an infinite number of poles in the w-plane. For the particular case where the medium is lossless, as is assumed in this paper, the poles lie on either the real or the imaginary axis. The pole locations are given by

$$w = \pm a_n \tag{A12}$$

where

$$\left.\begin{aligned} a_n &= \sqrt{\theta^2 - \left(\frac{n\pi}{d}\right)^2} \qquad \left(\theta^2 > \left(\frac{n\pi}{d}\right)^2\right) \\ a_n &= -j\sqrt{\left(\frac{n\pi}{d}\right)^2 - \theta^2} \qquad \left(\theta^2 < \left(\frac{n\pi}{d}\right)^2\right) \end{aligned}\right\} \tag{A13}$$

and where θ^2 is hereafter assumed to be a real quantity. As it turns out, this is the proper branch to choose to insure proper radiation requirements for large $|x|$.

APPENDIX A

The location of the poles as a function of the reflecting sheet distance d is of interest. Let N be the largest integer for which the following inequality is satisfied:

$$N < \frac{\theta d}{\pi} \tag{A14}$$

For the special case where $N = \left(\frac{\theta d}{\pi}\right)$, a pole lies at the origin. Furthermore, the pole lying at the origin is a pole of second order. However, for $N \neq \frac{\theta d}{\pi}$ for any reflecting sheet distance d, there are $2(N + 1)$ poles on the real axis. The poles at $w = \pm\theta$ remain fixed[5] as d is varied. However, as d is increased, the remaining poles migrate along the imaginary axis in toward the origin and out along the real axis toward the fixed poles, as indicated in figure 8. A more rigorous discussion of the behavior of $f(w)$ and $G(x)$ for large d is deferred to the end of this appendix.

For a given value of d, some of the poles lie on the real axis. Since the path of integration is along the real axis also, some modification is necessary before residue theory may be applied to evaluate the inverse transform. This modification may be made on a physical basis by assuming the medium to be slightly lossy. For the time dependence chosen, a lossy medium is characterized by the complex propagation constant

$$k = k' - jk'' \tag{A15}$$

where k' and k'' are real and positive. For a slightly lossy medium ($k' >> k''$), it can be shown that the real axis poles are shifted slightly off axis in a direction clockwise with respect to the origin of the w-plane. On the other hand, the imaginary axis poles are shifted in a direction counterclockwise with respect to the origin. Thus, in using residue theory to evaluate the integral in equation (A1), it will be assumed that the real axis poles are shifted slightly to avoid the integration path. However, residues are obtained under the assumption that these poles are on axis.

Integration contours in the complex w-plane for the evaluation of the integral in equation (A1) are as shown in figure 9. As can be seen from equation (A9), $f(w)$ has the proper behavior to assure that the contribution to the integral along each of the large semicircles is zero as the radius becomes infinite. By Cauchy's residue theorem

$$\left.\begin{aligned}
&\frac{1}{2\pi}\int_{-\infty}^{\infty} \frac{1}{k_z \tan(k_z d)}\, e^{-jk_x x}\, dk_x = \frac{1}{2\pi}\, 2\pi j \left(\text{sum of residues of } f(w)e^{-jwx} \text{ at upper half-plane poles of } f(w)\right) \quad (x < 0) \\
&\frac{1}{2\pi}\int_{-\infty}^{\infty} \frac{1}{k_z \tan(k_z d)}\, e^{-jk_x x}\, dk_x = -\frac{1}{2\pi}\, 2\pi j \left(\text{sum of residues of } f(w)e^{-jwx} \text{ at lower half-plane poles of } f(w)\right) \quad (x > 0)
\end{aligned}\right\} \tag{A16}$$

[5]The fixed poles represent the x-directed propagation constant for an infinite medium, that is, in the absence of the reflecting sheet.

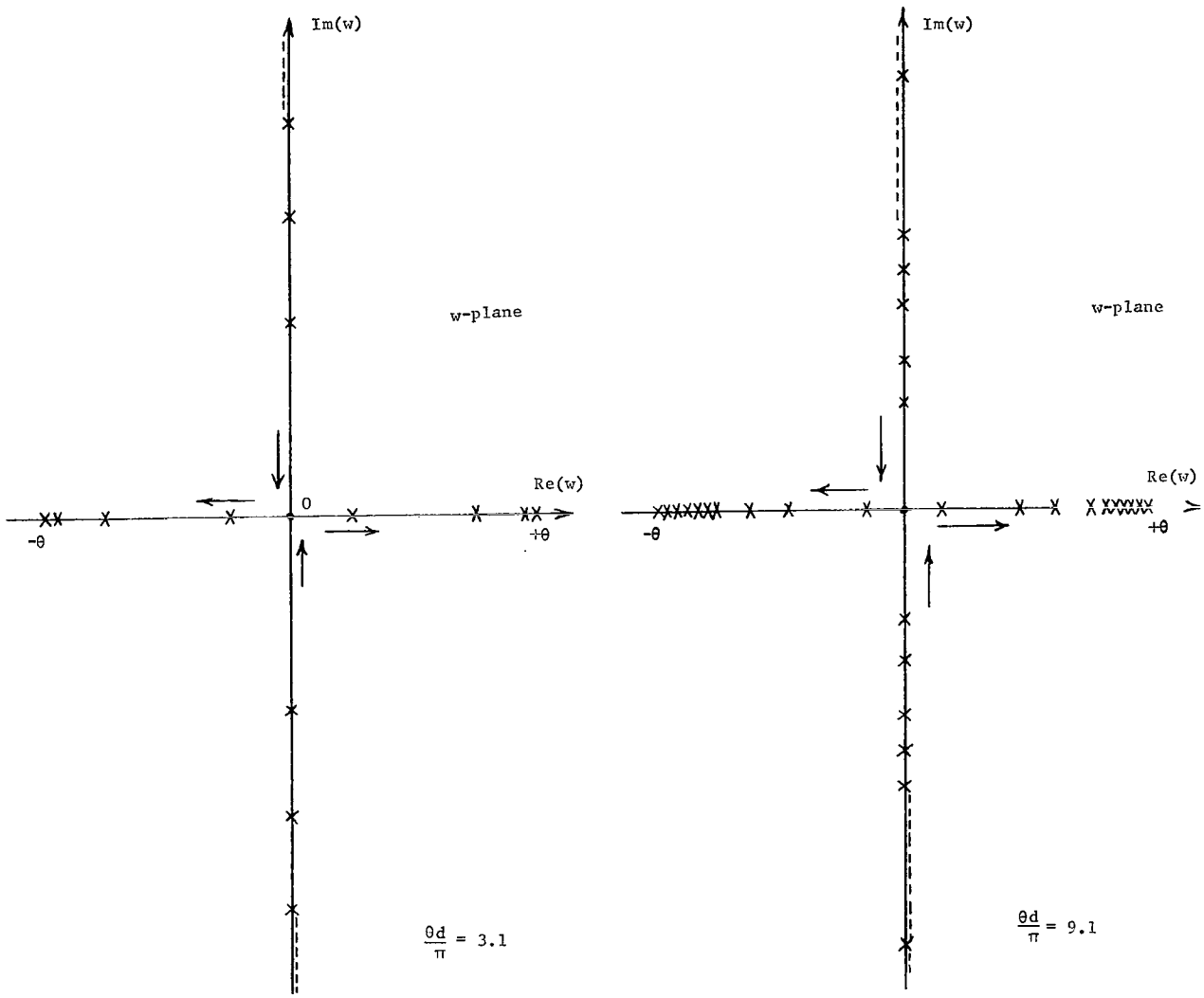

Figure 8.- Location of the poles of f(w) for two selected values of $\left(\frac{\theta d}{\pi}\right)$. The arrows indicate the direction of migration of the poles as d increases.

From equations (A6), (A12), (A13), and (A16), the residues Res are found to be

$$\text{Res}\left(\pm a_n\right) = \lim_{w \to \pm a_n}\left[(w \mp a_n)f(w)e^{-jwx}\right] = \mp \frac{e^{\mp j a_n x}}{a_n d\left(1 + \delta_o{}^n\right)} \tag{A17}$$

where $\delta_o{}^n$ is the Kronecker delta function defined in equation (33). Using equation (A17) in equation (A16) and combining the results yields

$$\frac{1}{2\pi}\int_{-\infty}^{\infty} \frac{1}{k_z \tan(k_z d)} e^{-jk_x x}\, dk_x = \frac{j}{d}\sum_{n=0}^{\infty} \frac{e^{-j a_n |x|}}{\left(1 + \delta_o{}^n\right) a_n} \tag{A18}$$

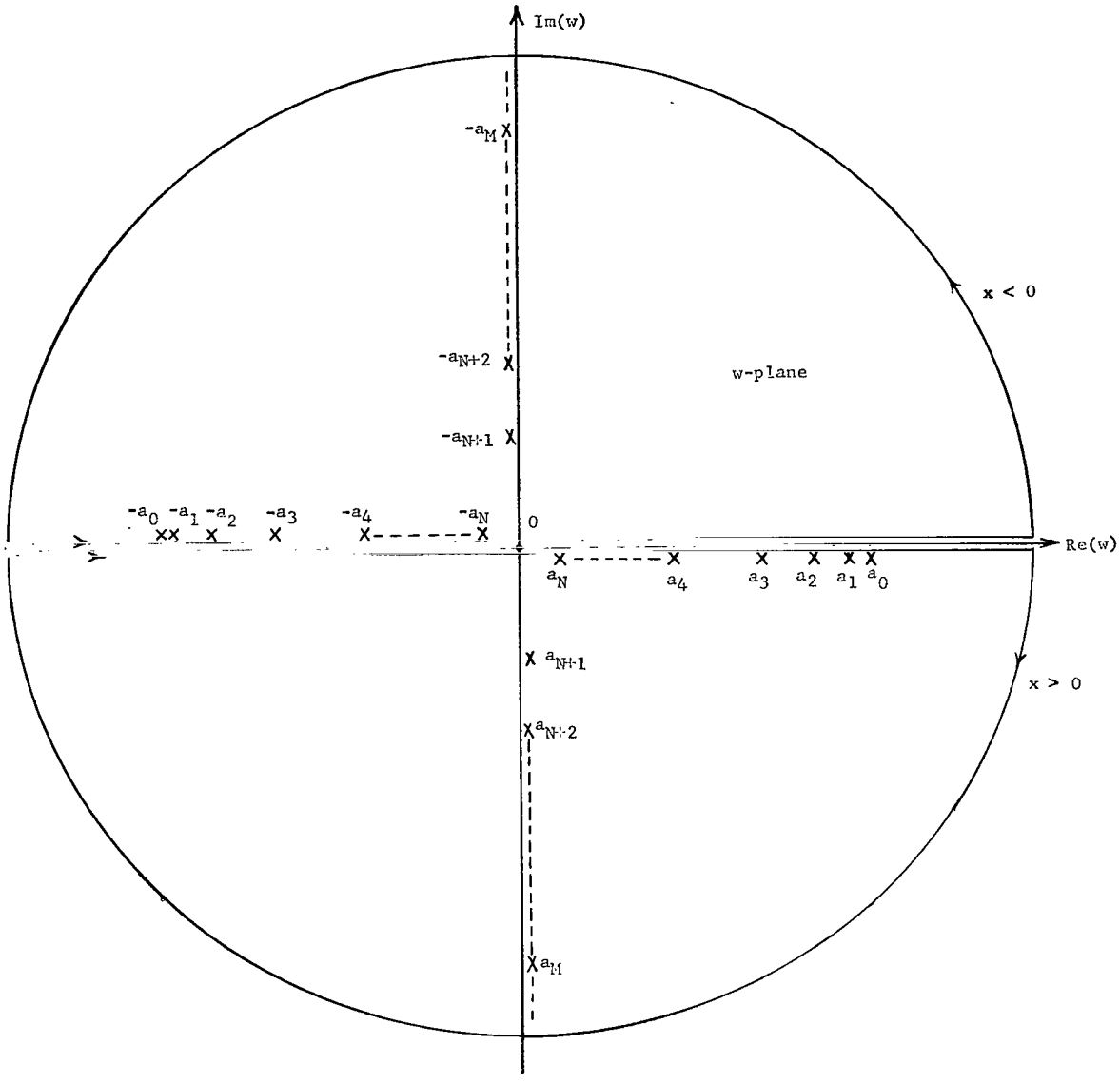

Figure 9.- Integration contours for G(x).

where the a_n are as given by equation (A13). This result is used in equation (B53). For the case where $k_y^2 = 0$, $\theta^2 = k^2$ in equation (A13). This result is used in equation (30).

An examination of the behavior of G(x) as the reflecting sheet spacing becomes infinite is facilitated by means of equation (A9). Use of equation (A9), for real w, in equation (A1) gives, after some manipulation,

APPENDIX A

$$G(x) = \frac{1}{2\pi}\int_{-\infty}^{\infty}\left[\frac{1}{\pi}\sum_{-\infty}^{\infty}\frac{1}{k_z^2 - \left(\frac{n\pi}{d}\right)^2}\frac{\pi}{d}\right]e^{-jk_x x}\,dk_x \tag{A19}$$

Let

$$h = \frac{n\pi}{d} \tag{A20}$$

then as n increases by unity,

$$\Delta h = (n+1)\frac{\pi}{d} - \frac{n\pi}{d} = \frac{\pi}{d} \tag{A21}$$

Thus, the sum in brackets becomes

$$\frac{1}{\pi}\sum_{-\infty}^{\infty}\frac{1}{k_z^2 - \left(\frac{n\pi}{d}\right)^2}\frac{\pi}{d} = \frac{1}{\pi}\sum_{-\infty}^{\infty}\frac{1}{k_z^2 - h^2}\Delta h \tag{A22}$$

As d approaches infinity, all the poles tend to approach the two fixed poles along the real axis in the w-plane and tend to become very closely spaced[6] in this region. The variable h thus becomes a continuous variable, Δh approaches dh, and the summation may be replaced by an integral.[7] Thus,

$$\lim_{\substack{d\to\infty \\ h\to 0}}\left[\frac{1}{\pi}\sum_{-\infty}^{\infty}\frac{1}{k_z^2 - \left(\frac{n\pi}{d}\right)^2}\frac{\pi}{d}\right] = \frac{1}{\pi}\int_{-\infty}^{\infty}\frac{dh}{k_z^2 - h^2} = \frac{2}{\pi}\int_0^{\infty}\frac{dh}{k_z^2 - h^2} \tag{A23}$$

Now

$$\frac{2}{\pi}\int_{-\infty}^{\infty}\frac{dh}{k_z^2 - h^2} = \frac{1}{\pi k_z}\log_e(-1) = \frac{j}{k_z} \tag{A24}$$

where the principal branch of the logarithm has been chosen. Using these results in equation (A19) yields

$$G(x) = j\frac{1}{2\pi}\int_{-\infty}^{\infty}\frac{e^{-jk_x x}}{k_z}\,dk_x \tag{A25}$$

---

[6]In light of the correlation of the work in this paper with the work of Compton (ref. 5), it is believed that, mathematically speaking, the fixed poles are converted to branch points as d approaches infinity.

[7]The approach used in converting the sum to an integral as d approaches infinity is similar to the approach taken by Knop (ref. 19, p. 537).

This integral has been evaluated by Compton (ref. 5, p. 24). Thus,

$$G(x) = \frac{j}{2} H_0^{(2)}(k|x|) \tag{A26}$$

Proceeding one step further, if equation (A26) is used in place of equation (A18) in equation (32), equation (35) becomes

$$Y = \frac{\omega\epsilon}{a} \int_0^a (a - x) H_0^{(2)}(kx)\, dx \tag{A27}$$

This result is identical to the expression of Compton (ref. 5, p. 25) for the aperture admittance of a parallel-plate waveguide radiating into an infinite lossless half-space.

APPENDIX B

THE APERTURE ADMITTANCE OF A RECTANGULAR WAVEGUIDE OPENING ON TO A PERFECTLY CONDUCTING GROUND PLANE AND ILLUMINATING A PERFECTLY CONDUCTING SHEET

The purpose of this appendix is to derive expressions similar to those in the text, when the parallel-plate waveguide is replaced by a TE_{10} mode-excited rectangular waveguide. The geometry of the problem is given in figure 10. The analytical approach to this problem is similar to the approach used in the text. The total aperture electric field is assumed to be the field of the dominant mode, that is, the TE_{10} mode. The aperture admittance is then found by finding an expression for the conjugate of the complex power flow through the aperture and dividing this result by the aperture voltage.

The fields in the region between the aperture and the reflecting planes may be expressed as a superposition of two sets of fields, one transverse electric (TE) and one transverse magnetic (TM) to the Z-axis. The fields may be generated by an electric vector potential function $\vec{F}(x,y,z)$ and a magnetic vector potential function $\vec{A}(x,y,z)$ given by

$$\vec{A}(x,y,z) = A_z(x,y,z)\hat{z} \tag{B1}$$

$$\vec{F}(x,y,z) = F_z(x,y,z)\hat{z} \tag{B2}$$

where $\hat{z}$ is a unit vector in the z-direction. The electric and magnetic field components are expressed in terms of the two potential functions. In particular,

$$E_x(x,y,z) = \frac{1}{j\omega\epsilon}\frac{\partial^2 A_z(x,y,z)}{\partial x\,\partial z} - \frac{\partial F_z(x,y,z)}{\partial y} \tag{B3}$$

$$E_y(x,y,z) = \frac{1}{j\omega\epsilon}\frac{\partial^2 A_z(x,y,z)}{\partial y\,\partial z} + \frac{\partial F_z(x,y,z)}{\partial x} \tag{B4}$$

$$H_y(x,y,z) = -\frac{\partial A_z(x,y,z)}{\partial x} + \frac{1}{j\omega\mu}\frac{\partial^2 F_z(x,y,z)}{\partial y\,\partial z} \tag{B5}$$

where the time dependence of $e^{j\omega t}$ has been chosen and where the Lorentz gage has been selected for both potential functions. The potential functions must satisfy the wave equations

$$\nabla^2\left[A_z(x,y,z)\right] + k^2 A_z(x,y,z) = 0 \tag{B6}$$

APPENDIX B

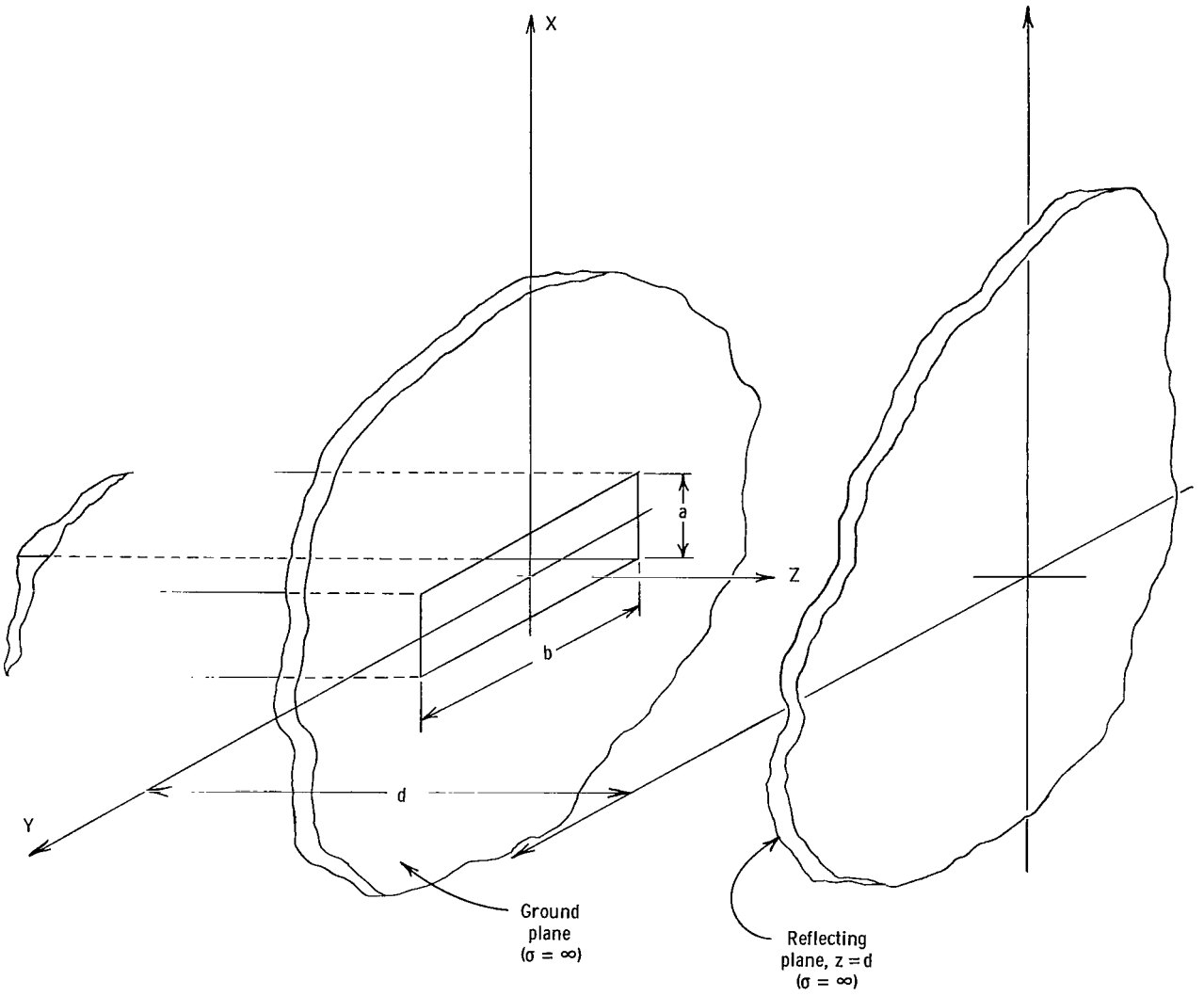

Figure 10.- The ground-plane-mounted rectangular waveguide illuminating a reflecting sheet.

$$\nabla^2\left[F_z(x,y,z)\right] + k^2 F_z(x,y,z) = 0 \tag{B7}$$

where

$$k^2 = \omega^2 \mu\epsilon \tag{B8}$$

and where ∇^2 denotes the Laplacian operator in rectangular coordinates.

The number of independent variables in each wave equation may be reduced from three to one by assuming double Fourier transform[8] solutions of the form

$$A_z(x,y,z) = \frac{1}{(2\pi)^2}\int\int_{-\infty}^{\infty} \overline{A}_z(k_x,k_y,z)\, e^{-jk_x x} e^{-jk_y y}\, dk_x\, dk_y \tag{B9}$$

$$F_z(x,y,z) = \frac{1}{(2\pi)^2}\int\int_{-\infty}^{\infty} \overline{F}_z(k_x,k_y,z)\, e^{-jk_x x} e^{-jk_y y}\, dk_x\, dk_y \tag{B10}$$

Substitution of equation (B9) into equation (B6) and equation (B10) into equation (B7) leads to the total differential equations

$$\frac{d^2\overline{A}_z(k_x,k_y,z)}{d_z^2} + k_z^2\overline{A}_z(k_x,k_y,z) = 0 \tag{B11}$$

$$\frac{d^2\overline{F}_z(k_x,k_y,z)}{d_z^2} + k_z^2\overline{F}_z(k_x,k_y,z) = 0 \tag{B12}$$

where

$$k_z^2 = k^2 - k_x^2 - k_y^2 \tag{B13}$$

---

[8]In this paper the double Fourier transform pairs $G(x,y,z)$ and $\overline{G}(k_x,k_y,z)$ are defined by the relations

$$G(x,y,z) = \frac{1}{(2\pi)^2}\int\int_{-\infty}^{\infty} \overline{G}(k_x,k_y,z)\, e^{-jk_x x} e^{-jk_y y}\, dk_x\, dk_y$$

$$\overline{G}(k_x,k_y,x) = \int\int_{-\infty}^{\infty} G(x,y,z)\, e^{jk_x x} e^{jk_y y}\, dx\, dy$$

Solutions of equations (B11) and (B12) are, respectively,

$$\overline{A}_z(k_x,k_y,z) = C_1(k_x,k_y)\, e^{jk_z z} + C_2(k_x,k_y)\, e^{-jk_z z} \tag{B14}$$

$$\overline{F}_z(k_x,k_y,z) = C_3(k_x,k_y)\, e^{jk_z z} + C_4(k_x,k_y)\, e^{-jk_z z} \tag{B15}$$

where $C_1(k_x,k_y)$, $C_2(k_x,k_y)$, $C_3(k_x,k_y)$, and $C_4(k_x,k_y)$ are arbitrary spectral constants to be determined from a knowledge of boundary conditions for the tangential electric field at both the aperture and reflecting planes. Substitution of equation (B14) into equation (B9), equation (B15) into equation (B10), and the results into equations (B3) to (B5) give the relations:

$$\overline{E}_x(k_x,k_y,z) = -\frac{k_x}{\omega\epsilon}\frac{d\overline{A}_z(k_x,k_y,z)}{dz} + jk_y\overline{F}_z(k_x,k_y,z) \tag{B16}$$

$$\overline{E}_y(k_x,k_y,z) = -\frac{k_y}{\omega\epsilon}\frac{d\overline{A}_z(k_x,k_y,z)}{dz} - jk_x\overline{F}_z(k_x,k_y,z) \tag{B17}$$

$$\overline{H}_y(k_x,k_y,z) = jk_x\overline{A}_z(k_x,k_y,z) - \frac{k_y}{\omega\mu}\frac{d\overline{F}_z(k_x,k_y,z)}{dz} \tag{B18}$$

where use of the Fourier transform definition has been made.

The aperture electric field is assumed to be the field of the TE_{10} mode with the electric field vector in the x-direction. Elsewhere on the aperture plane and over the entire reflecting plane, the tangential electric field components must vanish. Thus,

$$\left.\begin{aligned} E_x(x,y,0) &= V_o\sqrt{\frac{2}{ab}}\cos\left(\frac{\pi y}{b}\right) \qquad \left(|x| \leq \frac{a}{2};\ |y| \leq \frac{b}{2}\right) \\ E_x(x,y,0) &= 0 \qquad\qquad\qquad\qquad \left(|x| > \frac{a}{2};\ |y| > \frac{b}{2}\right) \end{aligned}\right\} \tag{B19}$$

and for all x and y

$$E_y(x,y,0) = E_x(x,y,d) = E_y(x,y,d) = 0 \tag{B20}$$

In the spatial frequency domain, the boundary conditions become

$$\left.\begin{aligned} \overline{E}_x(k_x,k_y,0) &= \int\int_{-\infty}^{\infty} E_x(x,y,0)e^{jk_x x}e^{jk_y y}\, dx\, dy \\ \overline{E}_x(k_x,k_y,0) &= \int_{-b/2}^{b/2}\int_{-a/2}^{a/2} V_o\sqrt{\frac{2}{ab}}\cos\left(\frac{\pi y}{b}\right)e^{jk_x x}e^{jk_y y}\, dx\, dy \end{aligned}\right\} \tag{B21}$$

or

$$\overline{E}_x(k_x,k_y,0) = 2\pi V_o\sqrt{2ab}\left(\frac{\sin\frac{k_xa}{2}}{\frac{k_xa}{2}}\right)\left[\frac{\cos\frac{k_yb}{2}}{\pi^2 - (k_yb)^2}\right] \tag{B22}$$

and

$$\overline{E}_y(k_x,k_y,0) = \overline{E}_x(k_x,k_y,d) = \overline{E}_y(k_x,k_y,d) = 0 \tag{B23}$$

Evaluation of equations (B16) and (B17) in the plane $z = d$ and application of equation (B23) lead to the system of simultaneous equations:

$$-\frac{k_x}{\omega\epsilon}\frac{d\overline{A}_z(k_x,k_y,d)}{dz} + jk_y\overline{F}_z(k_x,k_y,d) = 0 \tag{B24}$$

$$-\frac{k_y}{\omega\epsilon}\frac{d\overline{A}_z(k_x,k_y,d)}{dz} - jk_x\overline{F}_z(k_x,k_y,d) = 0 \tag{B25}$$

where $\frac{d\overline{A}_z(k_x,k_y,d)}{dz}$ and $\overline{F}_z(k_x,k_y,d)$ are unknown quantities. Similarly, at $z = 0$, one may establish the system of simultaneous equations

$$-\frac{k_x}{\omega\epsilon}\frac{d\overline{A}_z(k_x,k_y,0)}{dz} + jk_y\overline{F}_z(k_x,k_y,0) = \overline{E}_x(k_x,k_y,0) \tag{B26}$$

$$-\frac{k_y}{\omega\epsilon}\frac{d\overline{A}_z(k_x,k_y,0)}{dz} - jk_x\overline{F}_z(k_x,k_y,0) = 0 \tag{B27}$$

where $\frac{d\overline{A}_z(k_x,k_y,0)}{dz}$ and $\overline{F}_z(k_x,k_y,0)$ are the unknowns and where $\overline{E}_x(k_x,k_y,0)$ is given by equation (B22). Each of the two systems of simultaneous equations may be solved uniquely, inasmuch as $k_x \neq \pm jk_y$, to give the pairs of boundary conditions

$$\overline{F}_z(k_x,k_y,d) = 0 \tag{B28}$$

$$\frac{d\overline{A}_z(k_x,k_y,d)}{dz} = 0 \tag{B29}$$

$$\overline{F}_z(k_x,k_y,0) = -\frac{jk_y\overline{E}_x(k_x,k_y,0)}{k_x^2 + k_y^2} \tag{B30}$$

$$\frac{d\overline{A}_z(k_x,k_y,0)}{dz} = -\frac{\omega\epsilon k_x\overline{E}_x(k_x,k_y,0)}{k_x^2 + k_y^2} \tag{B31}$$

The four arbitrary spectral constants are determined upon application of equations (B28) to (B31) to equation (B14) and equation (B15). The results are

$$C_1(k_x,k_y) = - \frac{\omega\epsilon k_x \overline{E}_x(k_x,k_y,0)}{2k_z e^{jk_z d}\left(k_x^2 + k_y^2\right)\sin(k_z d)} \tag{B32}$$

$$C_2(k_x,k_y) = e^{j2k_z d} C_1(k_x,k_y) \tag{B33}$$

$$C_3(k_x,k_y) = - \frac{k_y k_z}{\omega\epsilon k_x} C_1(k_x,k_y) \tag{B34}$$

$$C_4(k_x,k_y) = \frac{k_y k_z e^{j2k_z d}}{\omega\epsilon k_x} C_1(k_x,k_y) \tag{B35}$$

Use of equations (B32) to (B35) in equation (B14) and equation (B15) and these results in equation (B18) gives the aperture magnetic-field transform in terms of the aperture electric-field transform. The result is

$$\overline{H}_y(k_x,k_y,0) = \frac{\left(k^2 - k_y^2\right)\overline{E}_x(k_x,k_y,0)}{j\omega\mu k_z \tan(k_z d)} \tag{B36}$$

The complex power flow through the aperture is

$$P = \int_{-b/2}^{b/2} \int_{-a/2}^{a/2} E_x(x,y,0)\, H_y^*(x,y,0)\, dx\, dy \tag{B37}$$

and the aperture admittance is given by

$$Y = \frac{P^*}{|V_o|^2} = \frac{1}{|V_o|^2} \int\int_{-\infty}^{\infty} E_x^*(x,y,0)\, H_y(x,y,0)\, dx\, dy \tag{B38}$$

where the limits of integration on x and y have been extended to infinity. This extension is permissible because $E_x(x,y,0)$ is zero on the ground plane; hence, the result is not affected. Parseval's theorem[9] is then used in equation (B38) to establish the relation

$$Y = \frac{1}{2\pi|V_o|^2}\int\int_{-\infty}^{\infty} \overline{E}_x^*(k_x,k_y,0)\,\overline{H}_y(k_x,k_y,0)\,dk_x\,dk_y \tag{B39}$$

Substitution of equation (B36) into equation (B39) gives

$$Y = \frac{1}{(2\pi)^2 j\omega\mu|V_o|^2}\int\int_{-\infty}^{\infty} \left|\overline{E}_x(k_x,k_y,0)\right|^2\left[\frac{k^2 - k_y^2}{k_z\tan(k_z d)}\right]dk_x\,dk_y \tag{B40}$$

and by use of equation (B19), this expression becomes

$$Y = \frac{2ab}{j\omega\mu}\int\int_{-\infty}^{\infty}\left[\frac{1}{k_z\tan(k_z d)}\right]\left\{\frac{\sin^2\left(\frac{k_x a}{2}\right)}{\left(\frac{k_x a}{2}\right)^2}\,\frac{\left(k^2 - k_y^2\right)\cos^2\left(\frac{k_y b}{2}\right)}{\left[\pi^2 - (k_y b)^2\right]^2}\right\}dk_x\,dk_y \tag{B41}$$

Parseval's theorem may be used on equation (B41). Let

$$\overline{G}_1(k_x,k_y) = \frac{1}{k_z\tan(k_z d)} \tag{B42}$$

---

[9]For the Fourier transform pair

$$G_1(x,y) = \frac{1}{(2\pi)^2}\int\int_{-\infty}^{\infty}\overline{G}_1(k_x,k_y)\,e^{-jk_x x}e^{-jk_y y}\,dk_x\,dk_y$$

$$G_2(x,y) = \frac{1}{(2\pi)^2}\int\int_{-\infty}^{\infty}\overline{G}_2(k_x,k_y)\,e^{-jk_x x}e^{-jk_y y}\,dk_x\,dk_y$$

Parseval's theorem is

$$\int\int_{-\infty}^{\infty} G_1(x,y)\,G_2^*(x,y)\,dx\,dy = \frac{1}{(2\pi)^2}\int\int_{-\infty}^{\infty}\overline{G}_1(k_x,k_y)\,\overline{G}_2^*(k_x,k_y)\,dk_x\,dk_y$$

APPENDIX B

$$\overline{G}_2{}^*(k_x,k_y) = \overline{G}_2(k_x,k_y) = \frac{\sin^2\left(\frac{k_x a}{2}\right)}{\left(\frac{k_x a}{2}\right)^2} \frac{\left(k^2 - k_y{}^2\right)\cos^2\left(\frac{k_y b}{2}\right)}{\left[\pi^2 - (k_y b)^2\right]^2} \tag{B43}$$

Then

$$G_2(x,y) = \frac{1}{(2\pi)^2} \int\int_{-\infty}^{\infty} \frac{\sin^2\left(\frac{k_x a}{2}\right)}{\left(\frac{k_x a}{2}\right)^2} \frac{\left(k^2 - k_y{}^2\right)\cos^2\left(\frac{k_y b}{2}\right)}{\pi^2 - (k_y b)^2} e^{-jk_x x} e^{-jk_y y}\, dk_x\, dk_y \tag{B44}$$

$$G_2(x,y) = \frac{1}{(2\pi)^2} \frac{4}{a^2} \left[\int_{-\infty}^{\infty} \frac{\sin^2\left(\frac{k_x a}{2}\right)}{k_x{}^2} e^{-jk_x x}\, dk_x\right] \left[\int_{-\infty}^{\infty} \frac{\left(k^2 - k_y{}^2\right)\cos^2\left(\frac{k_y b}{2}\right)}{\left[\pi^2 - (k_y b)^2\right]^2} e^{-jk_y y}\, dk_y\right] \tag{B45}$$

The integrals in brackets are evaluated by residue theory. They are identical to the integrals in Compton (ref. 5, pp. 64-65) and thus

$$G_2{}^*(x,y) = G_2(x,y) = \frac{1}{\pi^2 a^2}\, g(x)\, h(y) \tag{B46}$$

where

$$\left.\begin{aligned} g(x) &= \frac{\pi}{2}(a - |x|) \qquad \left(|x| \leq a\right) \\ g(x) &= 0 \qquad\qquad\quad \left(|x| > a\right) \end{aligned}\right\} \tag{B47}$$

$$\left.\begin{aligned} h(y) &= D_1(b - |y|)\cos\left(\frac{\pi y}{b}\right) + D_2 \sin\left(\frac{\pi |y|}{b}\right) \qquad \left(|y| \leq b\right) \\ h(y) &= 0 \qquad\qquad\qquad\qquad\qquad\qquad\qquad\quad \left(|y| > b\right) \end{aligned}\right\} \tag{B48}$$

and where

$$D_1 = \frac{1}{b^2}\left(\frac{k^2}{4\pi} - \frac{\pi}{4b^2}\right) \tag{B49}$$

$$D_2 = \frac{1}{\pi b}\left(\frac{k^2}{4\pi} + \frac{\pi}{4b^2}\right) \tag{B50}$$

Also

$$G_1(x,y) = \frac{1}{(2\pi)^2}\int\int_{-\infty}^{\infty} \frac{1}{k_z \tan(k_z d)} e^{-jk_x x} e^{-jk_y y}\, dk_x\, dk_y \tag{B51}$$

or

$$G_1(x,y) = \frac{1}{2\pi}\int_{-\infty}^{\infty}\left[\frac{1}{2\pi}\int_{-\infty}^{\infty} \frac{1}{k_z \tan(k_z d)} e^{-jk_x x}\, dk_x\right] e^{-jk_y y}\, dk_y \tag{B52}$$

The pairs of the integrand within brackets in equation (B52), namely, for $k_z = \pm\frac{n\pi}{d}$, give rise to specific modes which propagate in the $\pm x$-direction in the region between the aperture and the reflecting planes. Evaluation of this integral by residue theory (see appendix A) gives

$$\frac{1}{2\pi}\int_{-\infty}^{\infty} \frac{1}{k_z \tan(k_z d)} e^{-jk_x x}\, dk_x = \frac{j}{d}\sum_{n=0}^{\infty}\left[\frac{e^{-jk_x|x|}}{\left(1+\delta_o{}^n\right)k_x}\right] \tag{B53}$$

where the proper branch for k_x, namely,

$$\left.\begin{aligned} k_x &= \sqrt{k^2 - k_y{}^2 - \left(\frac{n\pi}{d}\right)^2} && \left(k^2 > k_y{}^2 + \left(\frac{n\pi}{d}\right)^2\right) \\ k_x &= -j\sqrt{\left(\frac{n\pi}{d}\right)^2 - k^2 + k_y{}^2} && \left(k^2 < k_y{}^2 + \left(\frac{n\pi}{d}\right)^2\right) \end{aligned}\right\} \tag{B54}$$

must be chosen to insure proper behavior of the fields for large $|x|$.

Substitution of equation (B53) into equation (B52) gives, after some manipulation,

$$G_1(x,y) = \frac{j}{2\pi d}\sum_{n=0}^{\infty}\left[\frac{1}{\left(1+\delta_o{}^n\right)}\int_{-\infty}^{\infty}\left(\frac{e^{-jk_x|x|}}{k_x}\right) e^{-jk_y y}\, dk_y\right] \tag{B55}$$

From Harrington (ref. 20)

$$\int_{-\infty}^{\infty} \frac{e^{-jk_x|x|}}{k_x} e^{-jk_y y}\, dk_y = \pi H_0{}^{(2)}\left(\rho\gamma_n\right) \tag{B56}$$

where

$$\left.\begin{aligned} \gamma_n &= \sqrt{k^2 - k_z^2} \qquad \left(k^2 > k_z^2\right) \\ \gamma_n &= -j\sqrt{k_z^2 - k^2} \qquad \left(k^2 < k_z^2\right) \end{aligned}\right\} \tag{B57}$$

$$k_z^2 = \left(\frac{n\pi}{d}\right)^2 \tag{B58}$$

$$\rho = \sqrt{x^2 + y^2} \tag{B59}$$

Thus equation (B55) becomes

$$G_1(x,y) = \frac{j}{2d} \sum_{n=0}^{\infty} \frac{1}{1 + \delta_o{}^n} H_0^{(2)}(\rho\gamma_n) \tag{B60}$$

Use of equations (B46) and (B60) in conjunction with Parseval's theorem and the properties of even functions gives

$$Y = \frac{16b}{a\omega\mu d} \sum_{n=0}^{\infty} \left[\frac{1}{1 + \delta_o{}^n} \int_0^b \int_0^a g(x)\, h(y)\, H_0^{(2)}(\rho\gamma_n)\, dx\, dy \right] \tag{B61}$$

This expression is separated into real and imaginary parts by use of the relation

$$H_0^{(2)}(-jx) = \frac{2j}{\pi} K_0(x) \tag{B62}$$

Thus

$$Y = G + jB \tag{B63}$$

where

$$G = \frac{16b}{a\omega\mu d} \sum_{n=0}^{N} \left[\frac{1}{1 + \delta_o{}^n} \int_0^b \int_0^a g(x)\, h(y)\, J_0\left(\rho\sqrt{k^2 - \left(\frac{n\pi}{d}\right)^2}\right) dx\, dy \right] \tag{B64}$$

APPENDIX B

$$B = -\frac{16b}{a\omega\mu d}\left\{\sum_{n=0}^{N}\left[\frac{1}{1+\delta_o{}^n}\int_0^b\int_0^a g(x)\,h(y)\,Y_0\left(\rho\sqrt{k^2-\left(\frac{n\pi}{d}\right)^2}\right)dx\,dy\right]\right.$$

$$\left.-\frac{2}{\pi}\sum_{n=N+1}^{\infty}\left[\frac{1}{1+\delta_o{}^n}\int_0^b\int_0^a g(x)\,h(y)\,K_0\left(\sqrt{\left(\frac{n\pi}{d}\right)^2-k^2}\right)dx\,dy\right]\right\} \tag{B65}$$

and where N is the largest integer for which

$$k^2 > \left(\frac{n\pi}{d}\right)^2 \tag{B66}$$

These expressions may be normalized by the choice of variables

$$x_\lambda = \frac{x}{\lambda} \tag{B67}$$

$$y_\lambda = \frac{y}{\lambda} \tag{B68}$$

The final results are

$$y = g + jb \tag{B69}$$

where

$$g = \frac{32\pi^3 b_\lambda}{a_\lambda d_\lambda}\sum_{n=0}^{N}\left[\frac{1}{1+\delta_o{}^n}\int_0^{b_\lambda} h(y_\lambda)\int_0^{a_\lambda} g(x_\lambda)\,J_0\left(2\pi\rho_\lambda\beta_n\right)dx_\lambda\,dy_\lambda\right] \tag{B70}$$

$$b = -\frac{32\pi^3 b_\lambda}{a_\lambda d_\lambda}\left\{\sum_{n=0}^{N}\left[\frac{1}{1+\delta_o{}^n}\int_0^{b_\lambda} h(y_\lambda)\int_0^{a_\lambda} g(x_\lambda)\,Y_0\left(2\pi\rho_\lambda\beta_n\right)dx_\lambda\,dy_\lambda\right]\right.$$

$$\left.-\frac{2}{\pi}\sum_{n=N+1}^{\infty}\left[\frac{1}{1+\delta_o{}^n}\int_0^{b_\lambda} h(y_\lambda)\int_0^{a_\lambda} g(x_\lambda)\,K_0\left(2\pi\rho_\lambda\alpha_n\right)dx_\lambda\,dy_\lambda\right]\right\} \tag{B71}$$

N is largest integer for which

$$N < 2d_\lambda \tag{B72}$$

and

$$\rho_\lambda = \sqrt{x_\lambda^2 + y_\lambda^2} \tag{B73}$$

$$\beta_n = \sqrt{1 - \left(\frac{n}{2d_\lambda}\right)^2} \qquad (n < 2d_\lambda) \tag{B74}$$

$$\alpha_n = \sqrt{\left(\frac{n}{2d_\lambda}\right)^2 - 1} \qquad (n > 2d_\lambda) \tag{B75}$$

$$g(x_\lambda) = a_\lambda - x_\lambda \tag{B76}$$

$$h(y_\lambda) = D_3(b_\lambda - y_\lambda)\cos\frac{\pi y_\lambda}{b_\lambda} + D_4 \sin\frac{\pi y_\lambda}{b_\lambda} \tag{B77}$$

$$D_3 = \frac{1}{8\pi^2 b_\lambda}\left(1 - \frac{1}{4b_\lambda^2}\right) \tag{B78}$$

$$D_4 = \frac{1}{8\pi^3 b_\lambda}\left(1 + \frac{1}{4b_\lambda^2}\right) \tag{B79}$$

REFERENCES

1. Redheffer, R. M.: Microwave Antennas and Dielectric Surfaces. J. Appl. Phys., vol. 20, no. 4, Apr. 1949, pp. 397-411.

2. Silver, Samuel, ed.: Microwave Antenna Theory and Design. Boston Tech. Publ., Inc., 1964.

3. Galejs, Janis: Admittance of a Waveguide Radiating Into Stratified Plasma. IEEE, Trans. Antennas Propagation, vol. AP-13, no. 1, Jan. 1965, pp. 64-70.

4. Villeneuve, A. T.: Admittance of Waveguide Radiating Into Plasma Environment. IEEE, Trans. Antennas Propagation, vol. AP-13, no. 1, Jan. 1965, pp. 115-121.

5. Compton, R. T., Jr.: The Admittance of Aperture Antennas Radiating Into Lossy Media. 1691-5, Dept. Elec. Eng., Ohio State Univ. Res. Found., Mar. 15, 1964.

6. Swift, C. T.; and Hodara, H.: Effects of the Plasma Sheath on Antenna Performance. Paper presented at AGARD/IRC Meeting on "Radio Wave Propagation Factors in Space Communications" (Rome, Italy), Sept. 1965.

7. Jones, James Earl: A Boundary Value Solution for an Infinite Parallel Plate Transmission Line Radiating Into a Lossy Half-Space. M. S. Thesis, Ohio State Univ., 1966.

8. Tsai, Leonard L.: The Reflection Coefficient of a TEM Mode Parallel-Plate Waveguide Illuminating a Perfectly Reflecting Sheet. 2143-1 (NASA Grant NGR-36-008-048), Dept. Elec. Eng., Ohio State Univ., Aug. 25, 1966.

9. Keller, Joseph B.: Geometrical Theory of Diffraction. J. Opt. Soc. Am., vol. 52, no. 2, Feb. 1962, pp. 116-129.

10. Ohba, Y.: On the Radiation Pattern of a Corner Reflector Finite in Width. IEEE, Trans. Antennas Propagation, vol. AP-11, no. 2, Mar. 1963, pp. 127-132.

11. Rudduck, R. C.: Application of Wedge Diffraction to Antenna Theory. NASA CR-372, 1966.

12. Nussenzveig, H. M.: Solution of a Diffraction Problem – I. The Wide Double Wedge, II. The Narrow Double Wedge. Phil. Trans. Roy. Soc. London, ser. A, vol. 252, no. 1003, Oct. 15, 1959, pp. 1-51.

13. Ghose, R. N.: Microwave Circuit Theory and Analysis. McGraw-Hill Book Co., Inc., 1963.

14. Culshaw, W.: Reflectors for a Microwave Fabry-Perot Interferometer. IRE, Trans. Microwave Theory Tech., vol. MTT-7, no. 2, Apr. 1959, pp. 221-228.

15. Culshaw, William: High Resolution Millimeter Wave Fabry-Perot Interferometer. IRE, Trans. Microwave Theory Tech., vol. MTT-8, no. 2, Mar. 1960, pp. 182-189.

16. Culshaw, William: Resonators for Millimeter and Submillimeter Wavelengths. IRE, Trans. Microwave Theory Tech., vol. MTT-9, no. 2, Mar. 1961, pp. 135-144.

17. Culshaw, William: Further Considerations on Fabry-Perot Type Resonators. IRE, Trans. Microwave Theory Tech., vol. MTT-10, no. 5, Sept. 1962, pp. 331-339.

18. Balanis, Constantine A.: Investigation of a Proposed Technique for Measurements of Dielectric Constants and Losses at V-Band Using the Fabry-Perot Principle. M.E.E. Thesis, Univ. of Virginia, 1966.

19. Knop, Charles M.: The Radiation Fields From a Circumferential Slot on a Metal Cylinder Coated With a Lossy Dielectric. IRE, Trans. Antennas Propagation, vol. AP-9, no. 6, Nov. 1961, pp. 535-545.

20. Harrington, Roger F.: Time-Harmonic Electromagnetic Fields. McGraw-Hill Book Co., Inc., c.1961.

NASA-Langley, 1968 —— 7 L-5645

"The aeronautical and space activities of the United States shall be conducted so as to contribute . . . to the expansion of human knowledge of phenomena in the atmosphere and space. The Administration shall provide for the widest practicable and appropriate dissemination of information concerning its activities and the results thereof."

—NATIONAL AERONAUTICS AND SPACE ACT OF 1958

NASA SCIENTIFIC AND TECHNICAL PUBLICATIONS

TECHNICAL REPORTS: Scientific and technical information considered important, complete, and a lasting contribution to existing knowledge.

TECHNICAL NOTES: Information less broad in scope but nevertheless of importance as a contribution to existing knowledge.

TECHNICAL MEMORANDUMS: Information receiving limited distribution because of preliminary data, security classification, or other reasons.

CONTRACTOR REPORTS: Scientific and technical information generated under a NASA contract or grant and considered an important contribution to existing knowledge.

TECHNICAL TRANSLATIONS: Information published in a foreign language considered to merit NASA distribution in English.

SPECIAL PUBLICATIONS: Information derived from or of value to NASA activities. Publications include conference proceedings, monographs, data compilations, handbooks, sourcebooks, and special bibliographies.

TECHNOLOGY UTILIZATION PUBLICATIONS: Information on technology used by NASA that may be of particular interest in commercial and other non-aerospace applications. Publications include Tech Briefs, Technology Utilization Reports and Notes, and Technology Surveys.

Details on the availability of these publications may be obtained from:

SCIENTIFIC AND TECHNICAL INFORMATION DIVISION

NATIONAL AERONAUTICS AND SPACE ADMINISTRATION

Washington, D.C. 20546